Global Biogeochemical Cycles

RESEARCH ARTICLE
10.1029/2022GB007636

Regional and Global Patterns of Apparent Organic Matter Reactivity in Marine Sediments

Philip A. Pika[1,2,3], Dominik Hülse[4,5], Timothy I. Eglinton[6], and Sandra Arndt[3]

[1]Department of Ecology, Faculty of Science, Charles University, Prague, Czechia, [2]Department of Earth Sciences, VU University of Amsterdam, Amsterdam, The Netherlands, [3]Biogeochemistry and Earth System Modeling, Geosciences, Environment and Society Department, Université Libre de Bruxelles, Brussels, Belgium, [4]Department of Earth Sciences, University of California, Riverside, CA, USA, [5]Max-Planck-Institute for Meteorology, Hamburg, Germany, [6]Department of Earth Sciences, ETH Zurich, Zurich, Switzerland

Key Points:

- We use an analytical diagenetic model to inversely determine organic matter (OM) reactivity in marine sediments on a global scale
- We provide transfer functions linking OM reactivity with oxygen uptake rates, total organic carbon content and water depth
- We present the first global map of benthic OM reactivity, which reflects observations and our current mechanistic understanding

Supporting Information:

Supporting Information may be found in the online version of this article.

Correspondence to:

P. A. Pika,
pikap@natur.cuni.cz

Citation:

Pika, P. A., Hülse, D., Eglinton, T. I., & Arndt, S. (2023). Regional and global patterns of apparent organic matter reactivity in marine sediments. *Global Biogeochemical Cycles*, *37*, e2022GB007636. https://doi.org/10.1029/2022GB007636

Received 7 NOV 2022
Accepted 17 MAY 2023

Author Contributions:

Conceptualization: Philip A. Pika, Sandra Arndt
Funding acquisition: Sandra Arndt
Methodology: Philip A. Pika, Dominik Hülse, Sandra Arndt
Project Administration: Sandra Arndt
Resources: Sandra Arndt
Software: Philip A. Pika, Dominik Hülse, Sandra Arndt
Supervision: Timothy I. Eglinton, Sandra Arndt
Validation: Dominik Hülse
Writing – original draft: Philip A. Pika, Sandra Arndt

Abstract Organic matter (OM) degradation in marine sediments is fundamental to understanding and constraining global biogeochemical cycling, whereby OM reactivity is at its core. Here, we use benthic diffusive oxygen uptake (DOU) rates as a proxy for OM reactivity. We apply an analytical diagenetic model to inversely determine OM reactivities in marine sediments (i.e., Reactive Continuum Model parameters a and ν) using data sets of global DOU, surface sediment OM contents, and seafloor boundary conditions. Simulated oxygen depth profiles show good agreement with observations, increasing confidence in our reactivity estimates. Inversely determined reactivities vary over orders of magnitude between individual sites ranging from high ($k = 0.252$ year^{-1}) for sediments in the Polar region to extremely low ($k = 7.96 \cdot 10^{-5}$ year^{-1}) in South Pacific. Our findings highlight the heterogeneity of OM reactivities, revealing regional patterns that broadly agree with observations and prior assessments. In general, high benthic reactivity can be linked to limited pelagic OM degradation favored by either a rapid vertical or lateral OM transport to the sediment or environmental factors, such as low oxygen concentrations or low temperature, slowing pelagic OM degradation. Finally, we develop a set of transfer functions that allow estimating OM reactivity as a function of DOU, OM content and water depths, and use one to derive the first global maps of benthic OM reactivity based on two global DOU maps. Despite the inherent observational biases in the data sets, our results provide a good first-order estimate of the apparent benthic OM reactivity agreeing with our current mechanistic understanding and observations.

Plain Language Summary The microbial degradation of organic matter (OM) in marine sediments is of considerable global importance for the nutrient and oxygen balance of the ocean. Simultaneously, OM burial in marine sediments represents an important sink for atmospheric CO_2. How susceptible OM is to degradation (i.e., its reactivity) represents arguably the most important parameter in diagenetic models. However, this reactivity is not globally uniform and depends on many controlling factors, making it notoriously difficult to define and represents a significant source of uncertainty in model estimates. Using an analytical diagenetic model, we inversely calculate the OM reactivity using global data sets of dissolved oxygen fluxes between the sediment and the overlying seawater. The resulting OM reactivities vary substantially, with high reactivities in polar marine sediments and low reactivities in sediments underlying the South Pacific. We observe that high OM reactivities coincide with accelerated lateral and/or vertical OM transport, low water column oxygen concentration or low water temperatures, while low OM reactivities coincide with low productivity, slow transport and remoteness from the coast. Finally, we construct a transfer function to provide the first global maps of benthic OM reactivity consistent with our existing mechanistic knowledge and observations.

1. Introduction

The heterotrophic degradation of organic matter (OM) in marine sediments is fundamental to understanding and constraining the role of the oceans in the global carbon cycle (Arndt et al., 2013; Burdige, 2007; Hedges & Keil, 1995). It is the engine behind the complex and dynamic suite of diagenetic processes in marine sediments and, thus, controls a plethora of different phenomena, such as benthic-pelagic exchange fluxes (Marcus & Boero, 1998; Ritzrau et al., 2001), the structure and functioning of the benthic ecosystem (Arnosti et al., 2011; Canfield, 1994), the dissolution and precipitation of minerals (Hales & Emerson, 1996), the size of gas and

Writing – review & editing: Philip A. Pika, Dominik Hülse, Timothy I. Eglinton, Sandra Arndt

gas hydrate reservoirs (Marquardt et al., 2010; Wadham et al., 2012), and carbon sequestration over geological timescales (Antia et al., 2001; Berner, 1990; Head et al., 2006). The degradation of OM in marine sediments is determined by the quantity and the quality of OM that settles onto the sediment (Arndt et al., 2013; LaRowe et al., 2020), which in turn is closely related to the delivery, production, transport and transformation of OM in the ocean. The susceptibility of OM toward microbial degradation during burial in the sediment depends on the interplay between a myriad of factors, including OM composition (Canuel & Martens, 1996; Dauwe et al., 1999; Hoefs et al., 2002; Zonneveld et al., 2010), availability of different terminal electron acceptors (TEAs) (Canfield, 1994; LaRowe & Van Cappellen, 2011), physical protection (Hemingway et al., 2019; Keil et al., 1994; Lalonde et al., 2012; Mayer, 1994), metabolic intermediates (Orcutt et al., 2013), microbial community structure (Arnosti et al., 2011; Canfield, 1994), temperature (Arnosti et al., 1998) or macrobenthic activity (Aller & Cochran, 2019). While the potential environmental controls on OM reactivity are increasingly well understood, their relative significance and how they interact to control apparent OM reactivity remains difficult to quantify. As a consequence, no mathematical framework currently exists to predict OM reactivity, and thus OM degradation dynamics, in marine sediments on a global scale.

Because benthic biogeochemical processes can be directly or indirectly traced back to OM degradation, observed sediment depth profiles of OM, TEAs and/or metabolic by-products are excellent indicators of OM reactivity (Canuel & Martens, 1996; Cowie et al., 1992; Dauwe et al., 1999; Toth & Lerman, 1977). However, the complex and dynamic interplay between diagenetic processes makes it often difficult to link them directly with OM degradation. For instance, depth profiles of sulfate concentration are not only influenced by organoclastic sulfate reduction, but also by anaerobic methane oxidation, sulfide re-oxidation by iron or manganese oxides, and oxygen (Van Cappellen & Wang, 1996). Therefore, integrated data-model approaches are traditionally used to disentangle this complex process interplay, quantify reaction rates and, ultimately determine apparent OM reactivities (e.g., Arndt et al., 2013). These approaches rely on Reaction-Transport Models (RTMs) that typically account for transport (advection, molecular diffusion, bioturbation, and bioirrigation) and reaction (production, consumption, equilibrium) processes. However, the applied RTMs may significantly vary in complexity (Arndt et al., 2013; Hülse et al., 2018; LaRowe et al., 2020). Apparent OM reactivity is generally considered a free parameter to fit observed depth profiles, reaction rates or sediment-water exchange fluxes. The growing number of individual RTM-based studies have not only improved our mechanistic understanding of the factors governing OM degradation dynamics in marine sediments (e.g., Arndt et al., 2009; Boudreau & Ruddick, 1991; Freitas et al., 2021; Soetaert et al., 1996a; Thullner et al., 2009), but also provided a growing global data set that facilitates assessment of large-scale patterns in apparent OM reactivity (Arndt et al., 2013; Boudreau, 1997; Boudreau & Ruddick, 1991; Emerson et al., 1985; Freitas et al., 2021; Middelburg, 1989; Stolpovsky et al., 2015; Toth & Lerman, 1977; Tromp et al., 1995).

Early studies used inversely determined OM degradation rate constants to derive global relationships between rates of OM degradation and a specific, readily observable quantity of the depositional environment, such as sedimentation rate or OM deposition flux (e.g., Boudreau & Ruddick, 1991; Emerson et al., 1985; Toth & Lerman, 1977; Tromp et al., 1995). These relationships were established based on a limited number of observations, generally covering a small number of depositional environments. In contrast, more recent studies, using a significantly larger and more diverse global set of OM rate constants, did not reveal statistically significant relationships between OM rate constant and sedimentation rate, water depth or OM deposition flux (Arndt et al., 2013; Freitas et al., 2021; LaRowe et al., 2020). Instead, they highlighted the highly heterogeneous nature of the dominant controls on apparent OM reactivity on all spatial scales. Nonetheless, a part of the large variability inherent to this global data set of OM degradation rate constants may actually stem from the use of different sampling techniques and/or model structures that limit the direct comparability of published estimates of apparent OM reactivity.

To our knowledge, only two inverse modeling studies used a common model structure and a coherent and also diverse set of sediment data, thereby maximizing the comparability of inverse estimates (Boudreau & Ruddick, 1991; Freitas et al., 2021). For example, Boudreau and Ruddick (1991) inversely fitted OM depth profiles to determine apparent OM reactivities (i.e., OM degradation model parameters) for several different sites spanning a range of depositional environments ($r^2 = 0.9$, $n = 9$). While a recent study by Freitas et al. (2021) uses OM, sulfate and methane depth profiles and, in particular, the location of the sulfate-methane transition zone (SMTZ) to inversely determine apparent OM reactivities across a wide range of different depositional environments. Results not only provide important insights into the magnitude of apparent OM reactivity, and its regional trends, but also shed light on potential environmental controls on apparent OM reactivity.

However, the paucity of comprehensive pore water profile data limits the number of apparent OM reactivity estimates. More widely available benthic flux observations offer an alternative because, just like benthic pore water profiles, benthic exchange fluxes (e.g., O_2, NO_3^-, SO_4^{2-}, Alkalinity, dissolved inorganic carbon) are driven by the complex interplay of diagenetic processes. In particular, benthic oxygen consumption rates are a widely measured and commonly used proxy for OM degradation rates (Andersson et al., 2004; Berner, 1980b; Emerson & Hedges, 2003; Glud, 2008; Jørgensen et al., 2022; Stolpovsky et al., 2015). They are typically quantified by sediment incubations, flux calculations based on oxygen penetration depth (OPD) profiles, or eddy covariance techniques (Glud, 2008, and references therein). In marine sediments, the consumption of oxygen and the resulting uptake of oxygen across the seabed are driven by the aerobic heterotrophic degradation of OM and the re-oxidation of reduced species released during subsequent suboxic/anoxic heterotrophic degradation, whereby their relative significance is highly variable (Glud, 2008; Jørgensen et al., 2022; Soetaert et al., 1996b). For instance, if oxygen penetrates deep into the sediment, the aerobic metabolic pathway dominates the overall OM degradation, and benthic oxygen uptake is a direct measure of aerobic degradation rates (Bourgeois et al., 2017; Glud, 2008; Jørgensen et al., 2022; Soetaert et al., 1996b). This is the case in deep-sea sediments underlying the oligotrophic central ocean gyres, where benthic OM input is small and oxygen diffuses down through the sediment column (D'Hondt et al., 2009, 2015; Fischer et al., 2009; Røy et al., 2012). However, in most marine environments, oxygen is quickly consumed in the very shallow sediment layers. Anoxic metabolic pathways dominate these environments, and oxygen consumption is thus also controlled by the re-oxidation of reduced species (Jørgensen & Kasten, 2006; Jørgensen et al., 2022; Thullner et al., 2009). Nevertheless, oxygen uptake remains a useful proxy of OM degradation rates but requires the assumption of a complete re-oxidation of reduced species in the sediment as well as constraints on OM stoichiometries and electron sinks such as N_2 release by denitrification (Glud, 2008; Jørgensen et al., 2022). In general, these assumptions are valid and pose little limitation for the use of oxygen uptake as a proxy for OM degradation rates (Bourgeois et al., 2017; Grebmeier et al., 2006; Jahnke, 1996; Martin & Bender, 1988; Sayles et al., 1996; Seiter et al., 2004, 2005a, 2005b; Soetaert et al., 1996a).

The dynamics and magnitude of oxygen uptake rates have been extensively studied across a wide range of depositional environments (Archer & Devol, 1992; Glud, 2008; Glud et al., 1994), and a number of global- and regional-scale benthic maps of oxygen uptake rates have been derived from these growing data sets (Bourgeois et al., 2017; Jørgensen et al., 2022; Seiter et al., 2005a, 2005b). In combination with reaction-transport modeling, such global data sets thus provide an opportunity to explore potential patterns in OM reactivity and relate them to common environmental drivers. For example, Stolpovsky et al. (2015) inversely fitted a RTM to 185 observed benthic oxygen and nitrate fluxes to derive fitting parameters for a prescribed power law representation of OM degradation. Based on these results, they derived a global relationship that quantitatively constrains the power law model parameters to describe the decrease in benthic OM degradation rate as a function of OM sedimentation rate. While this study helps to parameterize benthic OM degradation in global biogeochemical ocean models designed for the modern ocean, it does not directly provide mechanistic insight into the environmental and ecological controls on apparent OM reactivity. The derived power model remains highly parameterized to contemporary environments making it transferability to vastly different past and/or future environmental conditions uncertain.

In this present study, we determine the apparent reactivity of benthic OM across a wide range of depositional environments by inversely fitting a recently developed, one-dimensional analytical early diagenetic model (Hülse et al., 2018; Pika et al., 2021) to a global data set of 355 measured diffusive oxygen uptake (DOU) rates. We then explore regional and global patterns in apparent OM reactivity, assess apparent OM reactivity in the context of regional environmental conditions. The main aims of this study are to: (a) quantify apparent OM reactivity across a wide range of depositional environments, (b) identify potential environmental controls on apparent OM reactivity for each province and identify a set of environmental conditions that favor high or low apparent OM reactivity, (c) derive quantitative relationships that allow estimating apparent OM reactivity based on an available predictor variable for global upscaling, and (d) generate a global map of apparent OM reactivity in marine sediments.

2. Methods

We use the global diagenetic model OMEN-SED-RCM (Hülse et al., 2018; Pika et al., 2021) to quantify apparent OM reactivity for 355 individual sites covering a wide range of marine depositional environments (Figure 1) by

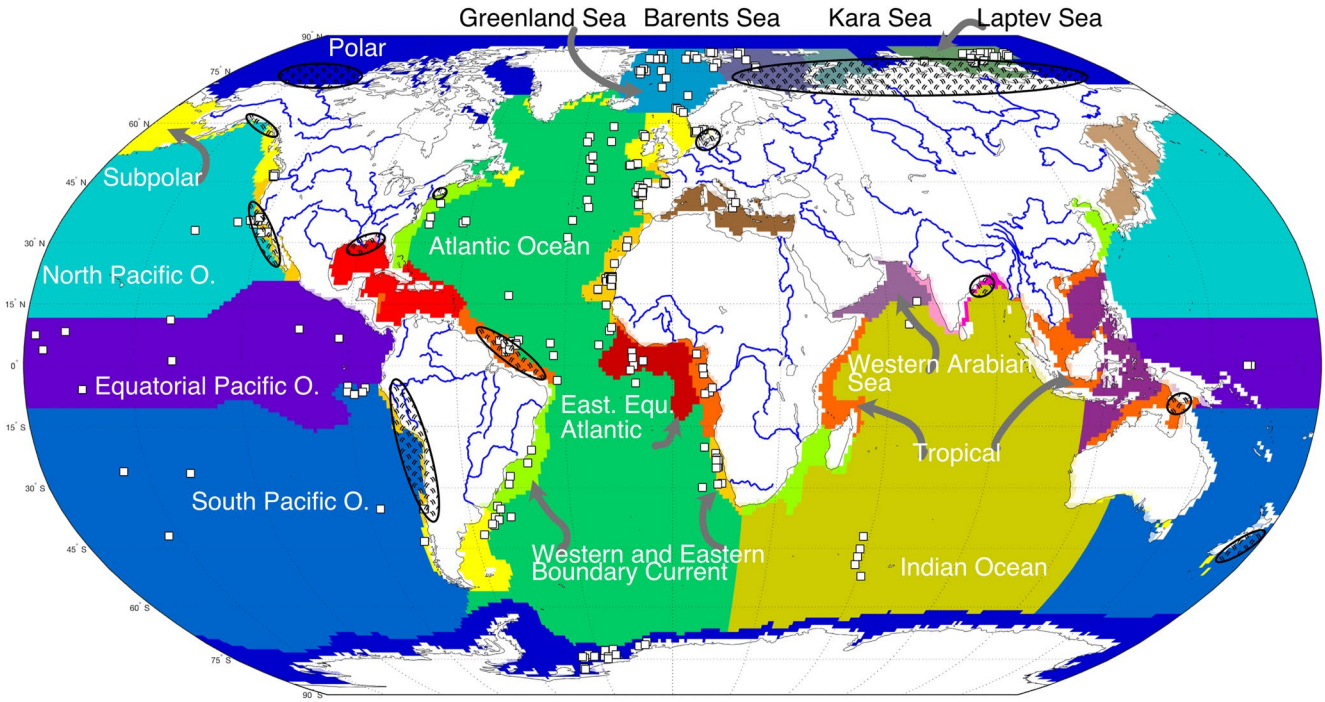

Figure 1. Benthic provinces (color-coded) and the location of data used in this study. White squares are locations of diffusive oxygen uptake (DOU) rate measurements used to estimate parameter *a*. Hotspots of intense burial and oxidation from Bianchi et al. (2018) are marked with patterned ovals. DOU sites are from Seiter et al. (2005a, 2005b).

inversely fitting observed benthic oxygen uptake rates. Benthic oxygen uptake is generally determined by three different approaches and is expressed as total oxygen uptake (TOU) or DOU depending on the measurement method (e.g., Jørgensen et al., 2022). TOU rates are determined by sediment core incubation or benthic chambers and, thus, account for benthic oxygen uptake by molecular diffusion, bioturbation and -irrigation, which is driven by benthic oxygen consumption through aerobic degradation and re-oxidation in the sediment, and fauna respiration. On the other hand, DOU rates are determined by simply applying Fick's law of diffusion or modeling oxygen consumption rates on the basis of measured oxygen depth profiles. DOU thus only accounts for the diffusive uptake of oxygen driven by the benthic oxygen consumption through aerobic degradation and re-oxidation in the sediment (Archer & Devol, 1992; Glud et al., 1994). Because the availability of information on macrobenthic activity and oxygen uptake rate is sparse and likely also highly variable in both time and space, we here use DOU rather than TOU observations to inversely fit OM degradation model parameters. DOU rates are generally calculated on the basis of measured oxygen (O_2) micro-scale depth profiles in the diffusive boundary layer (DBL) or the sediment using Fick's first law of diffusion (Glud, 2008). For sediment profiles:

$$DOU = \Phi \cdot D_s \frac{dO_2}{dz}, \quad (1)$$

where D_s (cm^2 s^{-1}) is the molecular diffusion coefficient D_0 (cm^2 s^{-1}) of oxygen corrected for tortuosity (compare (Hülse et al., 2018)), O_2 (mM) is the oxygen concentration, Φ is the porosity at the sediment-water interface (SWI) and z (cm) is the depth within the sediment (Glud et al., 1994; Jørgensen & Revsbech, 1985). If oxygen micro-scale profiles are directly measured in the DBL, the concentration gradient can simply be multiplied with the molecular diffusion coefficient.

2.1. Global DOU Data Set

The 355 individual DOU measurements used in this study are extracted from the global DOU data set compiled by Seiter et al. (2005a, 2005b) and complemented by additional measurements from the Southern Ocean (Schlüter, 1991), and from the oligotrophic South Pacific, where oxygen is known to diffuse down to the oceanic crust (D'Hondt et al., 2015, see also Figure 1). The resulting global DOU data set covers not only the entire ocean

hypsometry with 28 sites on the continental shelf (0–200 m), 254 sites on the continental slope (>200–3,500 m), and 110 sites in the deeper ocean (3,500–6,000 m), but also reflects a broad range of depositional environments (Figure 1). With the exception of some marginal seas (e.g., Kara and Bering Sea), all major ocean provinces are represented in the data set. Based on individual DOU measurements, Seiter et al. (2005a, 2005b) derived a globally extrapolated DOU map, presented as an estimated minimum particulate organic carbon flux to the sea floor (J_{OM}; 1° × 1° > 1,000 m sea floor depth (SFD), see Seiter et al. (2005a, 2005b), Jahnke (1996), Anderson and Sarmiento (1994)), by converting DOU to J_{OM}:

$$J_{OM} = DOU \cdot 0.77 \tag{2}$$

where the factor 0.77 represents the respiratory quotient that links oxygen consumption to organic carbon oxidation (106 mol C/138 mol O_2 = 0.77 C:O_2) derived from OM observations collected in mid- to deep sea marine sediment traps (Anderson & Sarmiento, 1994; Takahashi et al., 1985).

2.2. Diagenetic Model OMEN-SED-RCM

We use Organic Matter ENabled SEDiment model (OMEN-SED), a one-dimensional, analytical diagenetic model (Hülse et al., 2018) to inversely determine OM degradation model parameters (i.e., OM reactivity). OMEN-SED has recently been extended with a multi-G approximation of the reactive continuum model (RCM) of organic matter degradation (OMEN-SED-RCM; Pika et al., 2021). OMEN-SED-RCM is particularly suited for the inverse determination of OM reactivity parameters across many sites because it is computationally efficient and has been designed for global-scale applications. It explicitly describes the dynamics of OM and the globally most important TEAs (i.e., O_2, NO_3^-, SO_4^{2-}), and methane (CH_4), as well as the production and re-oxidation of reduced species (NH_4^+, H_2S). OMEN-SED(-RCM) is based on the vertically resolved conservation equation for solid and dissolved species in porous media (e.g., Berner, 1980a; Boudreau, 1997):

$$\frac{\partial \sigma C_i}{\partial t} = \frac{\partial}{\partial z}\left(D_{bio}\sigma \frac{\partial C_i}{\partial z} + D_i^* \sigma \frac{\partial C_i}{\partial z} \right) - \frac{\sigma \omega \partial C_i}{\partial z} + \alpha_i \sigma (C_{i,0} - C_i) + \sigma \sum_j s_i^j R^j \tag{3}$$

Here, C_i represents the concentration of species i, t denotes time, and z is the sediment depth. For solid species the porosity term is given by $\sigma = (1-\Phi)$, whereas for dissolved species porosity assumes $\sigma = \Phi$. The effective molecular diffusion coefficient of dissolved species i is given by D_i ($D_i = 0$ for solid species), D_{bio} represents the bioturbation coefficient, ω the sedimentation rate, and α_i denotes the bioirrigation coefficient ($\alpha_i = 0$ for solid species), and $C_{i,0}$ is the concentration of species i at the SWI. The sum of consumption/production process rates is given by $\Sigma_j s_i^j R^j$, where the stoichiometric coefficient of species i is given by s_i^j for the kinetically controlled reaction j, with rate R^j. The implemented reaction network considers the most important primary and secondary redox reactions, equilibrium reactions, mineral dissolution and precipitation, and adsorption and desorption processes affecting the dissolved and solid species that are explicitly resolved in the model. A comprehensive and detailed description of the original version of OMEN-SED (v1.0) can be found in Hülse et al. (2018). The following section provides a short overview of the description of OM and oxygen dynamics implemented in the model.

Organic matter degradation is described via a n-G-approximation of the RCM for OM degradation (Boudreau & Ruddick, 1991). The practical reason for choosing the RCM over the 2-G representation is that it captures OM dynamics on a wider range of time and depth scales while requiring constrains on only two free parameters (Boudreau & Ruddick, 1991). In addition, the RCM is in better agreement with our theoretical and qualitative understanding of the OM degradation process (Arndt et al., 2013). The RCM assumes an initial, continuous distribution of OM compounds over the reactivity spectrum that follows a Gamma distribution defined by the positive, free parameters a and ν that determine the overall OM reactivity, k, and its evolution with burial time, age(z), at depth z (Boudreau & Ruddick, 1991):

$$k(z) = \frac{\nu}{a + age(z)} \tag{4}$$

Parameter a (in units of time, here years) reflects the lifetime of the most reactive compounds in the initial OM mixture and controls the rate of reactivity decrease with sediment depth/burial age. The parameter ν determines the overall shape of the distribution of the organic compounds and thus their combined reactivity. Figure 3 illustrates the effect of different $a - \nu$ values on the evolution of the apparent bulk OM reactivity, $k = \nu/a$, with burial age/sediment depth. Combinations of low ν and high a indicate the initial dominance of less reactive compounds and result in an overall low reactivity and a slow decrease of OM reactivity with burial time/depth (Figures 3a and 3b). In

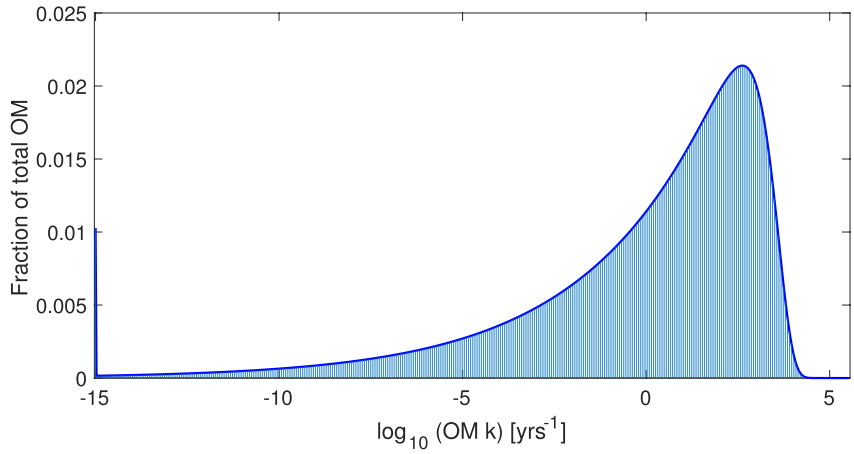

Figure 2. Multi-G approximation (blue bars) of the reactive continuum model (RCM, blue line) that is represented by the Gamma function. Idealized distribution of organic matter (OM) fractions for different OM reactivities assuming a RCM for OM degradation. This initial distribution (at $t = 0$) represents recently deposited OM (characterized by $a = 3 \cdot 10^{-4}$ and $\nu = 0.125$ Boudreau et al. (2008)).

contrast, high ν and low a values indicate the initial dominance of more reactive compounds and result in a higher overall reactivity and a rapid decrease in reactivity with burial time/depth (Figures 3a and 3b). OMEN-SED-RCM approximates the RCM by a multi-G model to enable the analytical solution of the set of coupled continuity equations (Figure 2). In other words, it approximates the continuous distribution of the bulk OM over the reactivity spectrum (fully determined by parameters a and ν) with a large number of discrete OM pools, OM_i. Each OM pool is degraded according to first-order kinetics with a degradation rate constant k_i (Figure 2) The apparent degradation rate constant of the bulk OM, $k(z)$, at sediment depth z (or at burial time age(z)) is given by:

$$k(z) = \Sigma k_i \cdot \frac{\mathrm{OM}_i(z)}{\mathrm{OM}(z)} = \frac{\upsilon}{a + age(z)} \tag{5}$$

For a given $a - \nu$ pair, the relative size of each OM fraction (i.e., at $z = 0$) is given by $f_i(0) = \mathrm{OM}_i(0)/\mathrm{OM}(0)$, and its reactivity $k_i(0)$ can be determined by dividing the continuous distribution of OM over the reactivity space into a number of discrete bins (see Pika et al., 2021). The minimum number of fractions, i, required to obtain a

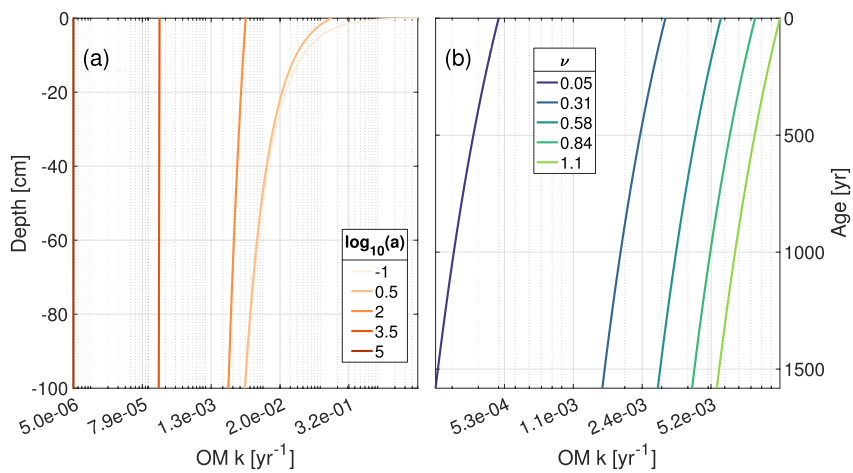

Figure 3. Depth/temporal evolution of the bulk organic matter (OM) reactivity dependent on the parameters of the gamma distribution for (a) constant $\nu = 0.5$ [−] and varying $a = 0.1 - 10^5$ years; and (b) varying $\nu = [0.05 - 1.1]$ [−] and constant $a = 100$ years. While parameter ν shifts the OM reactivity profile and does not change the shape (panel b), parameter a affects both the shape and the scale (panel a). The preferential degradation of more reactive types with increasing time/degradation results in a slowdown of OM consumption as only less reactive types remain in the sediment. This shift depends on the magnitude of the parameter a, showing how the sediment depth profile of OM depends on the apparent OM reactivity, $k(a, \nu)$. Apparent OM reactivity profiles are calculated assuming a sedimentation rate $\omega = 0.0645$ cm yr^{-1}.

close approximation of the RCM is determined by minimizing the error of the approximation to the continuous solution. Tests across a wide range of $a - \nu$ couples indicate that a minimum of 100 fractions are required to obtain an accurate approximation (approximation error <0.33% with 100 OM pools and <0.0134% with 500 OM pools Pika et al. (2021)). OMEN-SED-RCM then analytically solves the conservation equation for each OM pool—assuming steady-state conditions:

$$\frac{\partial \mathrm{OM}_i}{\partial t} = 0 = D_{\mathrm{OM}_i} \cdot \frac{\partial^2 \mathrm{OM}_i}{\partial z^2} - \omega \frac{\partial \mathrm{OM}_i}{\partial z} - k_i \cdot \mathrm{OM}_i \tag{6}$$

with $D_{\mathrm{OM}_i} = D_{bio}$ for $z \leq z_{bio}$ and $D_{\mathrm{OM}_i} = 0$ for $z > z_{bio}$ and $\mathrm{OM}_i = F(i) \cdot \mathrm{OM}_0$.

Oxygen, the most powerful oxidant among the TEAs (Kantor et al., 1992), is consumed first by the heterotrophic degradation of OM in shallow sediment layers. In addition, oxygen is consumed by the re-oxidation of reduced metabolites diffusing upward from the deeper anoxic sediment into the oxic zone (Aller, 1990; Boudreau & Canfield, 1993). These secondary reactions can represent a substantial fraction (up to ~56%, Jørgensen & Kasten, 2006) of the total oxygen consumption in marine sediments. To represent the most important oxygen sinks, we resolve the consumption of oxygen by both aerobic degradation of OM as well as the re-oxidation of produced ammonium, sulfide and methane (see also Hülse et al. (2018) for details). The differential equation to calculate oxygen concentrations is thus given by:

$$\frac{\partial O_2}{\partial t} = 0 = D_{\mathrm{O}_2} \cdot \frac{\partial^2 \mathrm{O}_2}{\partial z^2} - \omega \frac{\partial \mathrm{O}_2}{\partial z} - \frac{1-\phi}{\phi} \Sigma_i k_i \left[O_2 C + 2\gamma_{NH_4} NC_i \right] \cdot \mathrm{OM}_i(z) \tag{7}$$

where $O_2C = 138/106$ is the fixed C:O ratio, and γ_{NH_4} is a predefined fraction of ammonium produced during the aerobic degradation of OM that is directly nitrified to nitrate in the oxic zone (consuming 2 mol of oxygen per mole of ammonium produced). In addition, a sink term for oxygen is applied that implicitly accounts for oxygen consumption by the partial oxidation of ammonium and H_2S diffusing into the oxic zone from below (for more details, see Hülse et al., 2018).

2.3. Model Parametrization, Boundary Conditions and Forcing

We use the set of biogeochemical model parameters given in Hülse et al. (2018) (Tables 9 and 10) to reproduce a number of depth profiles observed across different depositional environments. RCM parameters a and ν are determined by inverse modeling as described in Section 2.4. In addition, OMEN-SED-RCM requires site-specific information for porosity, transport parameters, bottom water temperature, OM input, and the bottom water concentrations of the dissolved species of interest for our study (i.e., O_2, NO_3^-, SO_4^{2-}, CH_4, NH_4^+, H_2S). Bottom water temperature, oxygen and nitrate concentrations are constrained for each site using annually averaged observations reported for the deepest water depth recorded in the NOAA World Ocean Atlas 2016 (Lauvset et al., 2016). Bottom water ammonium, sulfide and methane concentrations are assumed to be zero due to the rapid oxidation of these species in oxygenated bottom waters. Bottom water sulfate concentrations are set to a globally constant value of 28 mM. Site-specific surface sediment organic carbon contents are taken from the data set assembled by Seiter et al. (2004). If no site-specific information is available, values from the geographically closest site reported in the above-mentioned data sets are used. The median distance between all DOU sites and the closest grid with surface sediment OC data is 0.03 km, with a minimum of 0 km and a maximum of 21 km.

OMEN-SED-RCM applies a constant porosity ϕ_0 throughout the sediment column to allow for the analytical solution of the coupled reaction-transport equations. Here we assign representative porosity values for shelf (0.45), slope (0.74) and abyssal sites (0.7) (Hantschel & Kauerauf, 2009; LaRowe et al., 2017). Site-specific bioturbation coefficients (D_{bio} in $\mathrm{cm^2\ yr^{-1}}$) are estimated using an empirically global relationship that allows estimating bioturbation coefficients as a function of seafloor depth (SFD) ($r^2 = 0.432$, $n = 132$, $p = 0.0000$; Middelburg et al., 1997):

$$D_{bio} = 5.2 \cdot 10^{(0.76241122 - 0.00039724) \cdot SFD} \tag{8}$$

An average global bioturbation depth, z_{bio}, of 10 cm (Boudreau, 1997) is assumed for all environments and SFD. For seafloor depths >5,000 m, bioturbation coefficients are set to zero to avoid instabilities in the analytical solution. Bioirrigation is described by multiplying the specific molecular diffusion coefficients $D_{mol,i}$ with an irrigation factor, f_{ir}, resulting in an apparent biodiffusion coefficient of:

$$D_{i,0} = D_{mol,i} \cdot f_{ir} \tag{9}$$

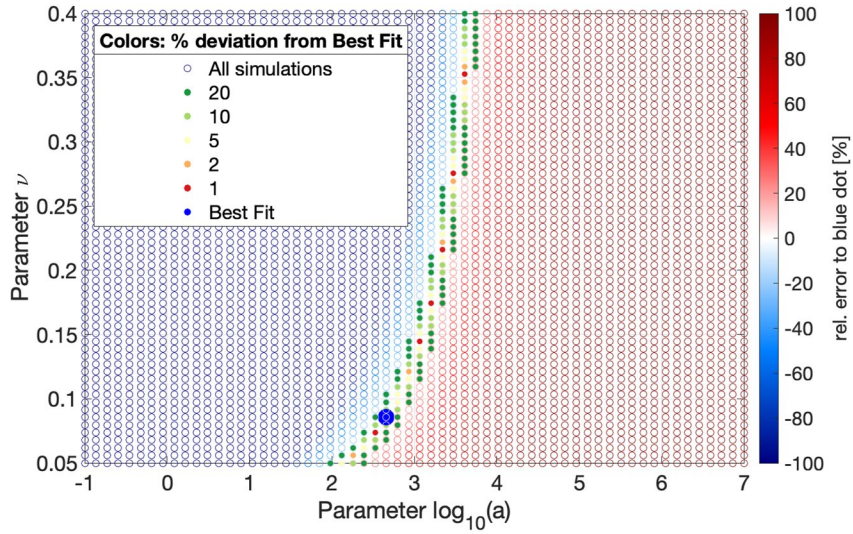

Figure 4. Sensitivity of simulated diffusive oxygen uptake (DOU) rates to variations in parameters a and ν over the entire range of previously published, model-derived $a - \nu$ pairs (Arndt et al., 2013). A hypothetical "measured" DOU rate of 0.75 mmol m^{-2} d^{-1}, which we aim to fit using Organic Matter ENabled SEDiment model, is marked with a filled blue circle. Variations from the hypothetical DOU rate by less than 1%, 2%, 5%, 10%, and 20% are given in red, orange, yellow, light and dark green filled circles, respectively. Variations of >20% are represented by open circles, and their magnitude is given by the color in the colorbar. Environmental characteristics: sea floor depth = 100 m; ω = 0.11 cm yr^{-1}; OC content = 2wt%. DOU = 0.75 mmol m^{-2} d^{-1}.

where $f_{ir} = 1$. The specific molecular diffusion coefficients $D_{mol,i}$ are corrected for sediment porosity ϕ and tortuosity F (expressed in terms of porosity, see Ullman & Aller, 1982) and are linearly interpolated for an ambient temperature T (in °C) using zero-degree coefficients D_i^0, temperature-dependent diffusion coefficients D_i^T:

$$D_{mol,i} = \left(D_i^0 \cdot D_i^T \cdot T\right) \cdot \frac{1}{\phi \cdot F} \tag{10}$$

See Hülse et al. (2018) and Soetaert et al. (1996a) for more details.

Sedimentation rates (ω in cm yr^{-1}) are estimated as a function of SFD using the empirical logistic equation of Burwicz et al. (2011)

$$\omega = \frac{w_1}{1 + \left(\frac{z}{z_1}\right)^{c_1}} + \frac{w_2}{1 + \left(\frac{z}{z_2}\right)^{c_2}} \tag{11}$$

applying the fitting parameters $w_1 = 117$ cm yr^{-1}; $z_2 = 4{,}000$ m; $w_2 = 0.006$ cm yr^{-1}; $c_1 = 3$; $z_1 = 200$ m; $c_2 = 10$.

2.4. Inverse Modeling Approach

We use OMEN-SED-RCM to determine apparent OM reactivity at selected sites in marine sediments by inversely fitting observed DOU rates. All inverse model fitting approaches of this type are limited by three main factors: core top loss, the effect of non-steady state conditions, and the uniqueness of the fit. While core top loss and non-steady state conditions may induce uncertainty to the inverse model results, the magnitude of uncertainty is comparable to those in non-site-specific model parameters, estimated transport parameters, and model forcing (see Section 2.3). More importantly, RCM parameters a and ν are essentially free parameters that determine the shape of the initial distribution of OM compounds over the reactivity continuum (Boudreau & Ruddick, 1991). Parameters a and ν are not completely independent, that is, a decrease in parameter ν (i.e., a decrease in apparent OM reactivity) might thus, to a certain degree, be compensated by a decrease in parameter a (i.e., an increase in apparent OM reactivity). Different pairs of $a - \nu$ may fit observed DOU rates equally well.

To evaluate the uniqueness of the inverse $a - \nu$ fit, we explore the variability of simulated DOU over the entire plausible $a - \nu$ space for a hypothetical depositional setting (Figure 4). The blue dot represents an arbitrarily

chosen DOU rate of 0.75 mmol m^{-2} d^{-1}. The colored bands highlight $a - \nu$ combinations for which simulated DOU rates deviate more than 1% from the reference DOU value of 0.75 mmol m^{-2} d^{-1}. Figure 4 shows that the inversely fitted $a - \nu$ combination is not unique. Results show that while a and ν are independent parameters, their effect on the resulting DOU rate is linked, that is, a decrease in parameter a (i.e., an increase in overall reactivity) is compensated by a decrease in ν (i.e., a decrease in overall reactivity). Several combinations of parameter a and ν can provide equally good fits to a reference DOU rate (dots of the same color in Figure 4). Hence, the DOU rate alone is insufficient to uniquely constrain both a and ν parameter values Additional site-specific information related to benthic OM degradation rates, such as porewater profiles or degradation rates, would be required to determine a truly unique fit. Unfortunately, this data is not available for our large DOU data set. However, Figure 4 also shows that simulated DOU values are more sensitive to variations in parameter a than ν. While the 1%–20% deviation band merely allows for variations in a within <1.5 orders of magnitude, it covers the entire plausible ν space.

At the same time, previously published model-derived continuum model parameters indicate that most of the global variability in apparent OM reactivity is controlled by variations in parameter a, while parameter ν remains largely constant (Arndt et al., 2013; Boudreau & Ruddick, 1991; Freitas et al., 2021; Middelburg, 1989). More specifically, a recent study compares inversely determined RCM parameter values on the global scale (Freitas et al., 2021) and reveals a-values varying from 10^{-3} to 10^{7} years while reported parameter ν-values mostly fall within a narrow range $0.1 < \nu < 0.2$ (see also Arndt et al., 2013; Boudreau & Ruddick, 1991). Exceptionally high values ($\nu \sim 1$) are reported for sites at the Peru Margin and the North Philippine Sea (Boudreau & Ruddick, 1991), and for the Bering Sea (Freitas et al., 2021). However, the authors suggested that these might be related to non-steady state depositional conditions. Therefore, we apply a constant ν value in OMEN-SED-RCM that is derived by averaging all published values ($\nu = 0.151 \pm 0.09$ for $n = 28$ results from Arndt et al. (2013) and Freitas et al. (2021). This value is also similar to the constant value of 0.16 applied in the empirically derived power law by Middelburg (1989).

We then use OMEN-SED-RCM to determine the optimal RCM parameter a for each of the 355 sites with observed DOU rates while keeping the RCM parameter $\nu = 0.151$ constant. We vary parameter a within a plausible range of $a \in [3.1 \cdot 10^{-4} - 10^{8}]$ years ($\Delta(\log(a)) = 0.02$) and determine its optimal value by minimizing the difference between simulated and observed DOU rates. Observed DOU rates range from a minimum rate of $\sim 10^{-4}$ mmol m^{-2} d^{-1} in the Southern Pacific Gyre to a maximum rate of ~28 mmol m^{-2} d^{-1} in the Eastern Boundary Current.

3. Results and Discussion

3.1. Evaluation of Model Performance in Capturing Local and Global Benthic Oxygen Dynamics

The performance of OMEN-SED(-RCM) in capturing diagenetic dynamics across a wide range of depositional settings has already been carefully assessed (see Hülse et al., 2018; Pika et al., 2021). Additionally to these test case studies, we here specifically evaluate and illustrate the ability of OMEN-SED-RCM to capture benthic oxygen dynamics on both local and global scale.

First, we assess the quality of our DOU fits by comparing observed oxygen depth profiles with those simulated by OMEN-SED-RCM using the best fit a-value for the specific site (Figure 5). Test sites where chosen on the basis of data availability and represent a diverse set of depositional environments: the Antarctic shelf and slope (PS1637-2, PS1611-4, PS1596-2, PS1595-2, and PS1645-2 (see Schlüter, 1991), the northern North Pacific (Stv 37/30 and Stv 31/14 (see Sauter et al., 2001) and the eastern tropical Atlantic (1B4-4 and 4IMP11 (see Jahnke et al., 1989). The inversely determined a-values generally capture the oxygen dynamics well. In particular, oxygen gradients and OPDs are well reproduced across a wide range of depositional settings without additional model tuning (Figure 5). The mismatch lies within the expected range and can be explained by local features in the bioturbation and -irrigation coefficients, which we approximate using global empirical relationships. Figure 5i also illustrates the effect of variations in apparent OM reactivity (i.e., $k = \nu/a$) on the simulated oxygen depth profile. An order of magnitude decrease in apparent OM reactivity (i.e., from $k = 0.151$ $year^{-1}$ to $k = 0.0151$ $year^{-1}$ or $a = [1 - 10]$ years, indicated by the gray lines) results in a change in OPD from 2 to 5 cm indicating that oxygen depths profiles would not allow constraining parameter a beyond the information already contained in the DOU rates.

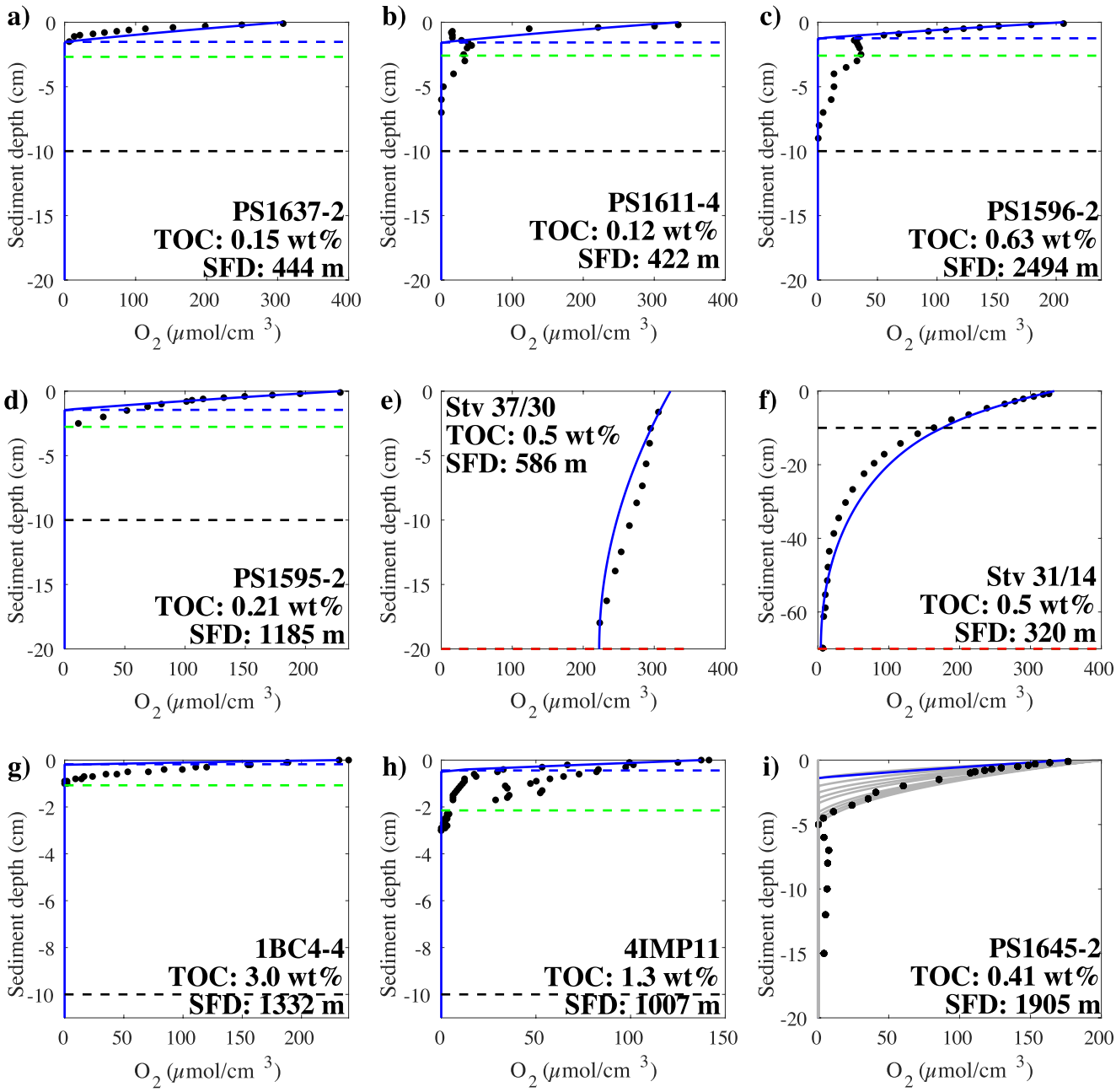

Figure 5. Observed (black circles) and simulated oxygen profiles using the optimal parameter *a* (blue lines) for (a–d) Antarctic shelf and slope (Schlüter, 1991), (e, f) northern North Atlantic (Sauter et al., 2001); (g, h) eastern tropical Atlantic Ocean (Jahnke et al., 1989); (i) Weddell Sea (Schlüter, 1991) shows multiple OMEN-SED-RCM oxygen profiles (in gray) simulated by different parameter *a* values (from unreactive (10 years) to reactive (1 year)) and illustrates the sensitivity of oxygen profile and oxygen penetration depth (OPD) to variations in apparent Organic matter reactivity. Horizontal dashed lines indicate the bioturbation depth, z_{bio} (black), the model calculated OPD (blue) and the nitrate penetration depth (profile not shown, green).

In addition, we further evaluate the inverse modeling results by the comparing 355 simulated OPDs with previously published global compilations of OPDs versus water depth (Figure 6). Observations show that OPD generally increases exponentially from a few millimeters in coastal sediments to several centimeters and even to several hundreds of meters in deep-sea sediments. Figure 6 shows that the 355 simulated OPDs capture this observed global trend well. Interestingly, inverse model results reveal a greater OPD variability with water depth than the smaller observational data set of Glud et al. (1994). This suggests that the OPD variability is not only controlled by benthic OM content (circle size in 6 (Glud et al., 1994)), but also by the apparent reactivity of that OM (see also Figure S3 in Supporting Information S1).

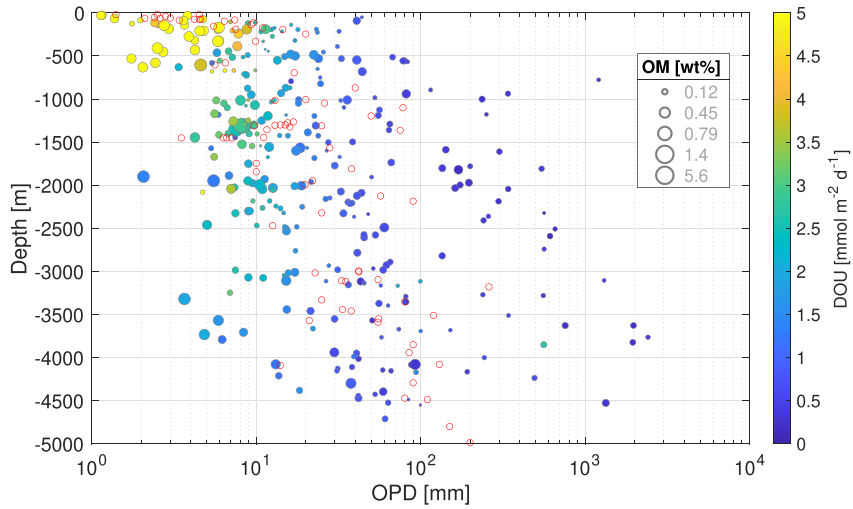

Figure 6. Observed (red circles) and simulated (colored circles) oxygen penetration depth (OPD) (OPD) over water depth. The marker size of the simulated OPD indicates surface sediment organic matter (OM) content, while its color indicates simulated diffusive oxygen uptake rates. The observational data (red circles) is extracted from the following literature: Jahnke et al. (1989), Canfield et al. (1993), Glud et al. (1994, 1998, 1999, 2003, 2009), Wenzhöfer, Adler, et al. (2001), Wenzhöfer, Holby, and Kohls (2001), Black et al. (2001), Giordani et al. (2002), Wenzhöfer and Glud (2002), Lansard et al. (2008, 2009), Sachs et al. (2009), Witte, Aberle, et al. (2003), Witte, Wenzhöfer, et al. (2003), Egger et al. (2018). See also Figure S2 in Supporting Information S1 illustrating the behavior of OPD with apparent OM reactivity (i.e., $k = \nu/a$).

3.2. Global Distribution of OM Reactivity Parameters

Figure 7 illustrates the distribution of inversely determined a values for the 355 specific sites and their average and standard deviation across the benthic provinces defined by Seiter et al. (2005a, 2005b).

In line with previously published observations and inversely determined OM reactivities (e.g., Arndt et al., 2013; Boudreau & Ruddick, 1991; Freitas et al., 2021), our results highlight the high intra- and inter-regional heterogeneity in apparent benthic OM reactivities driven by the complex and often very dynamic interplay of environmental factors that act in concert to control apparent OM reactivity in marine sediments. Site-specific, inversely determined parameters vary over orders of magnitude, reflecting very high ($k = 0.252$ year^{-1}; $a = 0.6$ years in the Polar region) to extremely low ($k = 6.3 \cdot 10^{-8}$ year^{-1}; $a = 2.4 \cdot 10^{6}$ years in the oligotrophic, central South Pacific) apparent OM reactivities. In addition, regionally averaged a-values mostly range from $k = 0.27$ year^{-1} to $7.96 \cdot 10^{-5}$ year^{-1} ($a = 5.6 \cdot 10^{-1} - 1.9 \cdot 10^{3}$ years) further confirming the higher frequency of a-values between 10^{0} and 10^{4} years, also observed by Freitas et al. (2021) (see Figure 7). Lastly, Figure 7 also reveals important differences in data availability across regions and its influence on the regional variability in parameter a. Well-studied regions, such as Eastern Boundary Systems, the Atlantic Ocean and Subpolar areas, display substantial interregional variability in determined a-values (i.e., a high standard deviation), which is of similar magnitude to the observed global variability.

3.3. Environmental Controls on Global Patterns in Benthic OM Reactivity

Despite the high variability, general regional patterns emerge from the inversely determined apparent OM reactivity estimates. These patterns, further corroborate and extend previously observed regional and global patterns (see Arndt et al., 2013; Freitas et al., 2021). In the following, we discuss the emerging trends in the context of their respective depositional environments with the aim of identifying potential dominant environmental controls on apparent OM reactivity.

3.3.1. Environmental Conditions Favoring High Benthic Apparent OM Reactivity ($k > 0.0151$ year^{-1}; $a < 10$ years)

The highest average apparent OM reactivities (i.e., $k > 0.0151$ year^{-1}; $a < 10$ years) are determined for the Western Arabian Sea (with $k = [0.22, 0.016]$ year^{-1}; $a = [0.7, 9.5]$ years, $n = 2$), the Polar ($\mu(k) = 0.059 \pm 0.069$ year^{-1}; $\mu(a) = 6.99 \pm 8.07$ years, $n = 20$) and Subpolar ($\mu(k) = 0.047 \pm 0.049$ year^{-1}; $\mu(a) = 8.36 \pm 8.44$ years,

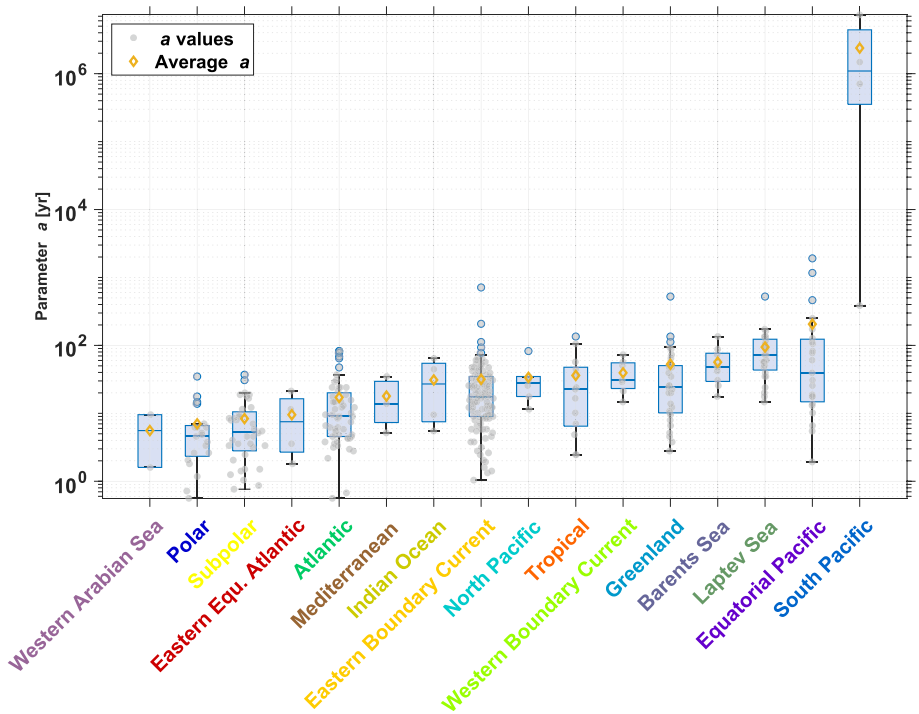

Figure 7. Boxplot for parameter a based on model fits to diffusive oxygen uptake (DOU) rates separated by benthic province. The red diamond represents the average $\log_{10}(a)$-values from the DOU fits ($n = 355$) for each province. For each boxplot the median value is the short horizontal bar within the rectangle, the bottom and top sides illustrate the 25th and 75th percentiles of the distribution, while the whiskers delineate interquartile range, and values beyond the whisker range (blue circles) are marked as outliers (i.e., 1.5 times distant from the interquartile range). The color of the province's name matches the color of the provinces in Figure 1. No data points available in the Kara Sea, the Sea of Japan and in the Caribbean Sea.

n = 37) province, and the Eastern Equatorial Atlantic (Congo deep-sea fan, $\mu(k)$ = 0.036 ± 0.035 year^{-1}; $\mu(a)$ = 9.53 ± 8.88 years, n = 6) (see Figures 1 and 7). Furthermore, individual sites in the Eastern Boundary Systems ($\mu(k)$ = 0.042 ± 0.032 year^{-1}; $\mu(a)$ = 5.5 ± 2.8 years, n = 33), the Western Equatorial Pacific ($\mu(k) = 0.055 \pm 0.055$ year^{-1}; $\mu(a) = 5.57 \pm 5.62$ years, $n = 2$), the Greenland province ($\mu(k) = 0.03 \pm 0.013$ year^{-1}; $\mu(a)$ = 5.76 ± 2.4 years, n = 7), and at sites underlying the Polar Front in the Indian Ocean province ($\mu(k) = 0.021 \pm 0.0082$ year^{-1}; $\mu(a) = 7.51 \pm 2.87$ years; $n = 2$) also display locally high apparent OM reactivities despite being characterized by regionally lower mean reactivities (i.e., $k < 0.015$ years^{-1}; $a > 10$ years, see Figure 7 and Figure S4a in Supporting Information S1). These high apparent OM reactivities are not only fully consistent with high, previously published model-derived reaction rate constants (Hartnett & Seitzinger, 2003; Lohse et al., 1998; Luff et al., 2000), but also with observational evidence, such as high OM reactivity. For instance, high benthic activity (Arnosti & Holmer, 2003; Boetius, Ferdelman, & Lochte, 2000; Boetius, Springer, & Petry, 2000; Fabiano & Danovaro, 1998; Mollenhauer et al., 2003, 2007; Nedwell et al., 1993; Ståhl et al., 2004), high benthic biomass (Gerdes et al., 1992; Piepenburg et al., 2002), elevated incubation rates (Koho et al., 2013), high DOU rates (Seiter et al., 2005a, 2005b) and shallow OPDs (Sachs et al., 2009; Schlüter, 1991).

A comparison of environmental conditions across these depositional environments reveals that, although the highest apparent OM reactivities are often found in depositional environments that are dominated by marine OM (i.e., the Weddell Sea sites (Polar province), the Arabian Sea, the Equatorial Pacific and the Eastern Boundary Upwelling systems), a regional prevalence of marine OM is not necessarily a pre-requisite for a high benthic OM reactivity. Regionally, high apparent OM reactivity is also determined for a number of continental margin systems that receive a more complex mix of both marine and terrestrial OM (i.e., the European shelf seas (Skagerrak, Celtic sea), the deep Southern Argentine basin, the southern Chile continental margin, the Washington margin off the coast of the Columbia River, and for the Congo deep-sea fan). Instead, comparing environmental conditions across these high reactivity regions reveals a set of recurring environmental conditions that coincide with high benthic OM reactivity. All of these environmental conditions exert a limiting effect on the heterotrophic degradation of settling OM in the water column and can be broadly divided into two groups of environmental controls.

The first group limits pelagic OM degradation by accelerating the transfer of OM to the sediment and, thus, reducing its residence time in the water column through: (a) the formation of large phytodetrital aggregates, (b) fronts, mesoscale eddies and ice edge effects, or (c) gravity-controlled, lateral mass flow processes. In particular, rapidly sinking large phytodetrital aggregates are widely observed in the high reactivity provinces (Beaulieu et al., 2013, and references therein). Such large phytodetrital aggregates are known to drive a rapid, pulsed deposition of largely undegraded OM to the sediment. For instance, in the Weddell Sea (Polar province), phytodetrital aggregates support strong, seasonal OM deposition pulses that represent >90% of the annual OM flux to the sediment (Palanques et al., 2002; Riebesell et al., 1991; Wefer & Fischer, 1991). In the Greenland/Norwegian Sea, high contents of algal pigment and the occurrence of thick phytodetritus layers on the sediment reveal an enhanced OM transfer efficiency due to the formation of post-bloom aggregates close to the ice edge off Greenland and on the Barents Sea slope (Graf, 1989; Graf et al., 1995; Pfannkuche, 1993; Ritzrau et al., 2001). Similarly, phytodetrital aggregates maintain high OM fluxes to great water depth in the Indian Ocean's polar front (Rabouille et al., 1998) and temporarily represent an important fraction of the total flux in the eastern Equatorial Pacific. The formation of such phytodetrital aggregates and subsequent mass sinking is favored by a high abundance and stickiness of phytoplankton cells, a reduced efficiency of the euphotic zone's food web and an increased turbulent fluid shear that can further enhance particle contact rates (Alldredge et al., 1995; Riebesell et al., 1991).

In addition, a number of physical processes, such as enhanced mixing, fronts, mesoscale eddies, and ice edge effects, can further accelerate the vertical transport of OM to the sediment. For instance, in the Arabian Sea and on the European Shelf, mixed layer deepening caused by winter cooling and wind mixing has been linked to peak OM deposition (Pfannkuche, 1993; Pfannkuche & Lochte, 2000). Similarly, mesoscale eddies forming seasonally in the coastal upwelling zone of the Arabian Sea enhance OM deposition (Honjo et al., 1999). Accelerated OM transport to the SWI has also been observed in connection with transport and subduction in mesoscale fronts that are commonly observed at the Polar Front (Indian Ocean), in eastern boundary and coastal upwelling systems (Kadko et al., 1991; Omand et al., 2015; Rabouille et al., 1998; Washburn et al., 1991). It is important to note that all of the above-discussed physical processes not only accelerate vertical transport but generally also facilitate the entrainment of nutrients into the euphotic zone, thus supporting high primary production rates and, sometimes the formation of phytodetrital aggregates. It is thus not easy to disentangle individual effects of phytodetrital aggregation and enhanced vertical transport processes.

Finally, accelerated lateral—rather than vertical—transport processes also support enhanced delivery of OM to the sediment. For instance, at the Argentine margin (subpolar province) and the Congo lobe sites (Eastern Equatorial Province), gravity-controlled mass flow processes accelerate the lateral transport of OM down the slope, creating local depo-centers that are hotspots of OM degradation (Hensen et al., 1998, 2000; Mollenhauer et al., 2003, 2007). For instance, the southern part of the Argentine margin is subject to large inputs of biogenic material from the Southern Ocean that is transported over long distances (up to 1,000 km, Benthien & Müller, 2000) by the strong western boundary current of Antarctic Bottom Water along the continental margin (Hensen et al., 2000). Intense gravity-controlled mass flow processes on the slope and benthic storms fueled by the high kinetic energy generation in the area of the Brazil-Malvinas Confluence create thick nepheloid layers and mud waves that affect the entire region. The strong downslope transport of fine-grained particles and organic-rich aggregates creates a depo-center on the slope (between 2,500 and 3,500 m.b.s.l.) characterized by high OM contents and benthic degradation rates (Mollenhauer et al., 2003, 2007). Similarly, the Congo River is directly connected to a submarine canyon system (Babonneau et al., 2002) that channels large amounts of terrestrial OM to the deeper ocean (Heezen & Hollister, 1964; Savoye et al., 2000, 2009) and supports the development of rich lobe ecosystems (Rabouille et al., 2017) and that are hotspots of OM degradation (Pozzato et al., 2017).

The second group of environmental controls that favors high benthic OM reactivity exerts a direct limiting effect on pelagic OM degradation rates. Here, two different controls emerge: (a) the presence of extended oxygen minimum zones (OMZ) in the water column in combination with oxygenated bottom waters and (b) low water column temperatures. For instance, the Arabian Sea, the Eastern Equatorial Pacific, and eastern boundary upwelling systems are all characterized by extensive OMZs sustained by the upwelling of more oxygen-depleted deep waters in combination with intense oxygen consumption fueled by high export production (Koho et al., 2013). The critical role of oxygen availability in controlling heterotrophic OM degradation rates has been widely demonstrated (Hedges & Keil, 1995; Hedges et al., 1999; Hulthe et al., 1998; Keil et al., 2004). Recently, inverse modeling of global pelagic degradation rates from assimilated satellite and oceanographic tracer observations showed a respective >30% and 80% decrease in pelagic degradation rates under hypoxic (<50 μM O_2) and

suboxic conditions (<5 μM O_2) (DeVries & Weber, 2017). Similarly, shipboard incubation experiments in the Arabian Sea revealed an even more pronounced (50%–60%) decrease in pelagic degradation rates with a decrease in pelagic oxygen concentrations from 100 to 40 μM (Keil et al., 2016). Laboratory experiments, biomarker analysis, and thermodynamic calculations indicate that the observed reduction in OM degradation under low oxygen conditions can be explained by a reduced susceptibility of the non-amino acid fraction toward degradation under suboxic/anoxic conditions (Devol & Hartnett, 2001; Hartnett et al., 1998; Kristensen & Holmer, 2001; Van Mooy et al., 2002).

Consequently, a greater fraction of the more reactive OM compounds escapes degradation in the water column, resulting in a higher apparent OM reactivity at the SWI. Observations from the Arabian Sea indeed show that OM settling through low oxygen waters, preserves its reactivity and exhibits a high reactivity upon deposition in oxic bottom water, but remains less reactive if deposited in sub/anoxic bottom waters (Koho et al., 2013; Moodley et al., 2011). In addition, inverse model results also reveal that high OM reactivity coincides with low water column temperatures at sites in the Weddell Sea (Polar province), in the Greenland Sea, and sites underlying the Polar Front in the Indian Ocean (Rabouille et al., 1998). This observation agrees well with the findings of DeVries and Weber (2017) who show that temperature controls the main global pattern of mesopelagic organic carbon transfer efficiencies. Similarly, laboratory experiments with phytoplankton aggregates and field observations reveal a high temperature sensitivity of degradation rates as reflected in q_{10} values of 3.3 and 3.7, respectively (Iversen & Ploug, 2013; Mazuecos et al., 2015). A possible explanation for the limiting effect of temperature on pelagic, but not benthic degradation rates comes from the analysis of the spectrum of enzymes hydrolyzing both polysaccharides and peptides in the water column and sediments at high latitudes. Results show that enzymatic capabilities in the water column are more limited than those in underlying sediment (Arnosti, 2008, 2015). Arnosti et al. (2011) report a decreasing spectrum of enzyme activities from low to high latitudes and Fabiano et al. (2000) report very low enzyme activities in the Antarctic water column. As a consequence, some organic compounds may escape pelagic degradation due to the lack of specific hydrolytic enzymes and then fuel more intense benthic degradation. In contrast to pelagic rates, benthic degradation rates observed in cold settings are not intrinsically slower than those measured in temperate or tropical environments (Arnosti et al., 1998; Glud et al., 1998; Jørgensen & Kasten, 2006; Knoblauch et al., 1999; Sagemann et al., 1998; Thamdrup & Fleischer, 1998a, 1998b). This seemingly contradictory observation may result of the more stable bottom water temperatures as opposed to the seasonally changing water column temperatures that allow a better physiological adaption of the benthic microbial community to the permanently cold environmental conditions (e.g., Robador et al., 2009). This is further supported by high benthic extracellular enzyme activities observed in Antarctic sediments (Cho & Azam, 1988; Grossart & Ploug, 2001; D. C. Smith et al., 1992) which allow the benthic community to exploit episodic OM pulses rapidly (Fabiano & Danovaro, 1998; Sachs et al., 2009).

3.3.2. Environmental Conditions Favoring Intermediate Benthic Apparent OM Reactivity ($0.015 < k < 0.0015$ years^{-1}; 10 years $< a <$ 100 years)

Intermediate benthic OM reactivities are primarily found on dynamic continental margins (see Figure 7 and Figure S4b in Supporting Information S1), such as the Eastern Boundary Current systems ($\mu(k) = 0.017 \pm 0.024$ year^{-1}; $\mu(a) = 31.01 \pm 70.91$ years, $n = 110$), the Tropical region ($\mu(k) = 0.017 \pm 0.021$ year^{-1}; $\mu(a) = 36.11 \pm = 41.42$ years, $n = 13$), the Western Boundary Current systems ($\mu(k) = 0.005 \pm 0.003$ year^{-1}; $\mu(a) = 39.4 \pm 21.1$ years, $n = 7$), the Barents Sea ($\mu(k) = 0.0037 \pm 0.0023$ year^{-1}; $\mu(a) = 56.6 \pm 36.9$ years, $n = 9$) and the Laptev Sea ($\mu(k) = 0.0029 \pm 0.0024$ year^{-1}; $\mu(a) = 94.4 \pm 95.3$ years, $n = 28$). These inversely determined reactivities are in good agreement with previously published estimates of $\mu(a) = 79.8 \pm 80.4$ years (Arndt et al., 2013), including the California upwelling area with $a = 60$ (Marquardt et al., 2010; Middelburg, 1989), the Benguela upwelling area with $a = 43$ years (Marquardt et al., 2010) and the Humboldt upwelling area with $a = 98.9$ years (Middelburg, 1989). Continental margin provinces are complex and dynamic depositional systems influenced by a mixture of different OM sources, high sediment loads, complex circulation patterns, and intense erosion and deposition cycles (Blair & Aller, 2012). In particular, strong mineral protection (Aller & Blair, 2006; Blair & Aller, 2012; Keil et al., 1994; Mayer, 1994), intense pelagic degradation in mobile nepheloid layers and/or high sediment reworking rates resulting in multiple deposition/erosion cycles associated with strong bottom currents (Bao et al., 2018; Inthorn et al., 2006; Mollenhauer et al., 2003, 2007) that act to reduce apparent OM reactivity.

Intermediate OM reactivities are also determined for continental slopes adjacent to productive margins, such as the deep Argentine basin sites ($\mu(k) = 0.041 \pm 0.066$ year^{-1}; $\mu(a) = 24.6 \pm 24.3$ years, $n = 13$). Here, benthic

storms and intermediate nepheloid layers form around the shelf edge and upper slope and laterally transport material along isopycnals surfaces. Furthermore, high kinetic energy related to the Brazil-Malvinas Confluence may also induce benthic storms (Hollister & McCave, 1984). High benthic OM contents and benthic degradation rates are observed on the slope at water depths between 2,500 and 3,500 m where winnowing via the downslope transport of fine grained particles and organic-rich aggregates creates a depo-center at greater water depths (Mollenhauer et al., 2003, 2007).

Contrary to the traditional view that benthic OM reactivity decreases with water depth, our results indicate that not all deep-sea sediments are characterized by a low apparent OM reactivity. For instance, we estimate intermediate—and thus higher than expected—apparent OM reactivities ($k = 0.015 - 0.0015$ years^{-1}; $a = 10^1 - 10^2$ years) for sediments underlying the open Atlantic and North Pacific Oceans. These comparably high apparent OM reactivities generally coincide with either an efficient lateral or vertical transport of OM to the deep ocean (Mollenhauer et al., 2007). Both the North Pacific and Atlantic Ocean are comparably narrow ocean basins with a higher margin to open ocean ratio (Levin & Gooday, 2003). Mass wasting events such as collapse and slumping of sediments (Levin & Gooday, 2003), nepheloid boundary layers (Inthorn et al., 2006; Mollenhauer et al., 2007), earthquake-induced turbidity flows (e.g., Thunell et al., 1999), and strong bottom water currents or benthic storms (Hollister & McCave, 1984) efficiently redistribute sediment and OM to the deep ocean adjacent to the productive continental slopes (Levin & Gooday, 2003). This shallow to deep lateral transport is especially intense in regions of deep western boundary currents, recirculation, and high surface eddy kinetic energy over strong thermohaline bottom flows (McCave, 2019). The important role of lateral transport in supporting comparably high benthic OM reactivity in these abyssal sediments is further supported by observational evidence. For instance, a significant contribution of laterally transported OM to the overall deposition flux has been reported for all of the identified intermediate benthic reactivity sites in the deep Atlantic Ocean (Dickson & McCave, 1986; Lohse et al., 1998; Mollenhauer et al., 2005, 2007; Ohkouchi, 2002). Furthermore, Seiter et al. (2005a, 2005b) showed that DOU-OM data for the Northeast Pacific reveals a close relation to the adjacent Northwest American Continental Margin. Next to intense lateral transport, rapid, pulsed vertical transport also may result in intermediate benthic OM reactivity at abyssal sites. Many deep-sea sites, particularly in the temperate North Atlantic, are characterized by intense, seasonal spring/summer phytoplankton blooms and associated intense pulses of large phytodetritus aggregates that are efficiently transported to the seafloor (Lampitt & Antia, 1997; Longhurst & Glen Harrison, 1988; Longhurst et al., 1995). Patchy and often thick layers of green fluff have been frequently observed in the Porcupine Abyssal Plain, in the BIOTRANS area around the Mid-Atlantic Ridge and on the slope off south of New England (Levin & Gooday, 2003; Pfannkuche, 1993; Rice et al., 1991; Thiel, 1988). In addition, large phytodetrital aggregates have also been episodically observed on the deep seafloor adjacent to the California margin (C. R. Smith, 1992; K. L. Smith et al., 1994, 2013), where they provide a pulsed input of relatively reactive OM, which is reflected in the comparably high OM degradation rate constants (k = [0.083–4.97] year^{-1}) (Murray & Kuivila, 1990). Finally, the availability of biomineral bound OM (e.g., in opal or biogenic carbon shells) in the open ocean close to continental margins serves as a vector shielding reactive OM during transit from the surface to the deep sea. Upon reaching undersaturated deep waters, these nitrogen-rich vessels dissolve releasing the reactive OM (Arnarson & Keil, 2007).

3.3.3. Environmental Conditions Favoring Low ($k < 0.0015$ year^{-1}; $a > 100$ years) to Extremely Low ($k < 0.00015$ year^{-1}; $a > 1{,}000$ years) Benthic Apparent OM Reactivity

We determine the lowest apparent OM reactivities for deep-sea sediments underlying the oligotrophic, South Pacific central gyre (k = [$3.93 \cdot 10^{-4}$, $1.0 \cdot 10^{-7} - 2.06 \cdot 10^{-8}$] year^{-1}; a = [384, 1481046.0 − 7348872.8] years, $n = 4$, see Figure 7; Figure S4c in Supporting Information S1) that are also characterized by extremely low observed DOU rates (DOU = [$5.5 \cdot 10^{-5} - 1.7 \cdot 10^{-4}$] mmol m^{-2} d^{-1}) and OM contents (OC = [0.17–0.8] wt%). Our estimated OM reactivities are consistent with extremely low heterotrophic degradation rates, previously published low apparent OM reactivities (Røy et al., 2012) and deep OPD (D'Hondt et al., 2015; Murray & Grundmanis, 1980). The south Pacific is dominated by a large, anticyclonic subtropical gyre that creates an extended area of downwelling and, thus, oligotrophic conditions, resulting in low primary production and low vertical OM deposition fluxes (~0.3 gC m^{-2} yr^{-1}, i.e., roughly 1/30 of benthic OM deposition on the Californian slope Seiter et al. (2005a, 2005b), Longhurst et al. (1995)). In addition, the south Pacific is Earth's largest oceanic province (~10% of Earth's surface) and most locations are remote from continents or more productive shelf areas that could laterally supply OM (Kim et al., 2020). This remoteness also leads to a lack of mineral dust ballast, which otherwise promotes rapid transit through the long column of oxygen-rich water (Hartnett et al., 1998; Hedges & Keil, 1995).

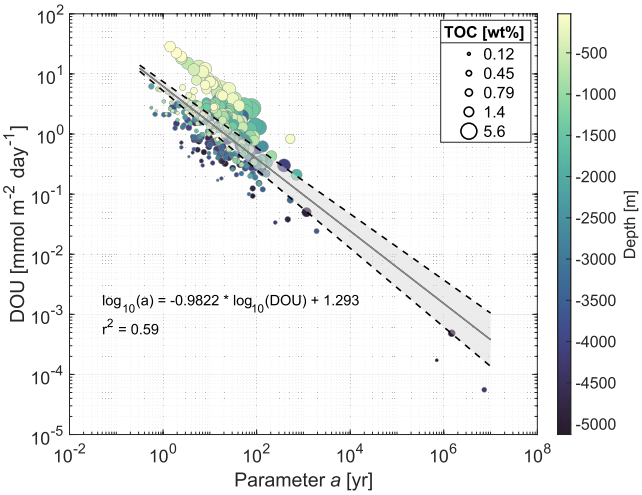

Figure 8. Observed diffusive oxygen uptake rates as a function of inversely determined apparent organic matter (OM) reactivity (i.e., $k = \nu/a$). The gray continuous line indicates the linear regression using Equation 12, the dashed lines and the gray area represent the 95% confidence interval. Additional information about the sampling sites are plotted as circle size (i.e., surface sediment OM wt%) and color (i.e., water depth).

Therefore, the small amounts of OM which ultimately reaches the sediment is extensively degraded (Hartnett et al., 1998; Hedges & Keil, 1995), resulting in low benthic OM reactivities. Although direct observations from beneath central ocean gyres are scarce, it is likely that these extremely low apparent OM reactivities of the central Atlantic and Indian oceans. Based on observations from the South Pacific gyres, D'Hondt et al. (2015) estimate that oxygen penetrates though the entire sediment column beneath in 9%–37% of the ocean's and 15%–44% of the Pacific's seafloor. These estimates are further supported by the absence of a SMTZ in these areas (Egger et al., 2018; LaRowe et al., 2020). Global maps of estimated oxygen penetration and SMTZ depths may thus serve as an initial guides to delineate the extent of such central ocean gyre, low OM reactivity zones.

In addition, to these extremely low apparent OM reactivities, low apparent OM reactivities ($k < 0.0015$ year^{-1}; $a > 10^2$ years) are determined for individual sites in the outer areas of the wide Arctic shelf of the Laptev Sea, the Western Equatorial Pacific, the Canary Current (off Northwest Africa), the California Upwelling Current (Northwest America) area, and for sites within the deeper, central regions of the Norwegian Greenland Sea (Figure 7). These low apparent OM reactivities highlight the large inter-regional variability of OM reactivity on the seafloor. Low reactivity sites within these regions are generally associated with more oligotrophic conditions in an otherwise productive depositional environment or an enhanced influence of pre-degraded material to the more distal parts of the lateral OM transport pathways from shelf to slope. For instance, the more oligotrophic Western Equatorial Pacific and offshore the Eastern Boundary Upwelling systems reveal lower apparent OM reactivity. Similarly, the deeper, central regions of the Norwegian Greenland Sea, such as the Vøring Plateau (950–1,450 m.b.s.l.), the East Greenland Basin (3,000 m.b.s.l.) and the Lofoten Basin (3,300 m.b.s.l.) are characterized by lower pigment contents, and low DOU and degradation rates (Bourgeois et al., 2017; Graf et al., 1995), indicative of less reactive OM reaching the sediment in the deeper parts of the Norwegian Greenland Sea. On the Arctic shelf, outer shelf and slope sites are generally characterized by low primary production rates and low OM deposition fluxes (Bourgeois et al., 2017; Harada, 2016), and low concentrations of reactive OM compounds and low extracellular enzyme activities (Boetius & Damm, 1998), explaining the low apparent OM reactivities determined for these sites (Bröder et al., 2018).

3.4. Transfer Functions Predicting OM Reactivity Parameter *a*

Modeling results highlight the strong link between observed DOU rates, surface sediment OM contents and inversely determined apparent OM reactivities (i.e., $k = \nu/a$) for the 355 sites explored in this study (Figure 8). Our findings reveal a moderately robust inverse relationship in form of a power law (linear on a log-log scale) between DOU rate and apparent OM reactivity (Figure 8, $r^2 = 0.59$ for $a = f(\mathrm{DOU})$):

$$\log_{10}(a) = -0.9822 \cdot \log_{10}(DOU) + 1.293 \quad (12)$$

whereby parameter a is given in years and DOU rate in mmol m^{-2} d^{-1}. Figure 8 illustrates that the very low reactivity sites in the South Pacific gyre (i.e., very high parameter a) strongly influence the regression model. However, they represent an important, yet underrepresented endmember in the global DOU data set. Integrating these values helps to remove some of the observational biased toward more biogeochemical active regions and ensures that the empirical relationship covers a wide range of environmental conditions encountered at the global ocean seafloor.

Adding surface sediment OM content (in wt%) as explanatory variables to Equation 12 further improves the regression model to explain up to 82% of the variability ($r^2 = 0.82$ for $a = f(\mathrm{DOU}, \mathrm{OM})$):

$$\log_{10}(a) = 0.74 + 0.524 \cdot OM - 1.23 \cdot \log_{10}(DOU) \quad (13)$$

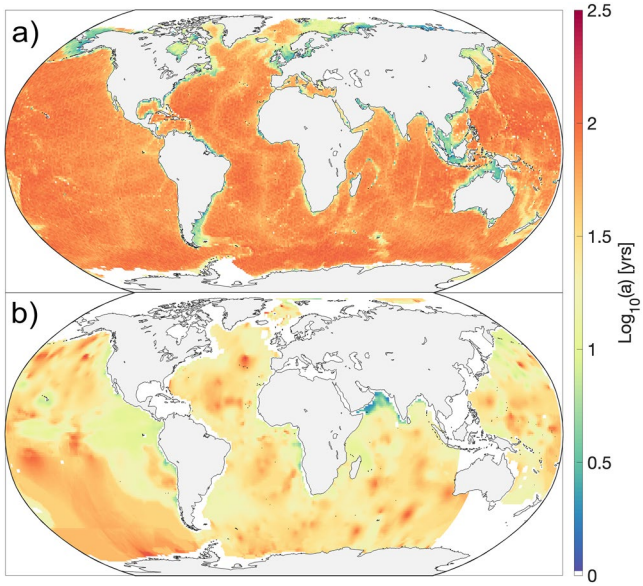

Figure 9. Global map of estimated apparent organic matter (OM) reactivity (i.e., $k = \nu/a$) calculated as a function of diffusive oxygen uptake with Equation 12. Panel (a) uses data from Jørgensen et al. (2022), and panel (b) uses data from Seiter et al. (2005a, 2005b). The white areas indicate lack of data to estimate OM reactivities. Note that the parameter a is displayed on a logarithmic scale. See Figure S1 in Supporting Information S1 for the respective maps.

Finally, the quality of the fit can be further increased by also adding seafloor depth, SFD (in m), as an explanatory variable. In this case, the empirical equation explains 92% of the observed variability ($r^2 = 0.92$ for $a = f$(DOU, OM, SFD)):

$$\log_{10}(a) = 1.0957 - 0.00015 \cdot SFD + 0.51 \cdot OM - 1.441 \cdot \log_{10}(DOU) \quad (14)$$

Adding additional environmental factors, such as sedimentation rate, bottom water oxygen content or the intensity of macrobenthic activity do not improve the fit.

3.5. Global Distribution of Benthic OM Reactivity Parameter *a*

The global transfer functions (Equations 12–14) derived above can be used to predict the spatial distribution of apparent OM reactivities (i.e., $k = \nu/a$) on the global ocean seafloor from data sets of DOU rate, surface sediment OM content (e.g., Atwood et al., 2020; Jørgensen et al., 2022; Lee et al., 2019; Seiter et al., 2005a, 2005b), and SFD. However, currently available global data products are often highly correlated. For instance, the global DOU rate map proposed by Seiter et al. (2005a, 2005b) is derived by applying several empirically derived regional DOU-OM relationships from a surface sediment OM map that, in turn, is based on a combination of qualitative and quantitative geostatistical observations. On the other hand, the global DOU map presented by Jørgensen et al. (2022) is derived by applying an empirically derived relationship linking log-transformed oxygen uptake with SFD and net primary production (NPP) to gridded global data sets of SFD and NPP. Using highly correlated input variables (i.e., DOU and OM content, DOU and SFD) to extrapolate a third parameter (i.e., apparent OM reactivity) would render such extrapolation highly sensitive to the ratio of the two input parameters (which is indeed observed here; results not shown). Consequently, Equations 13 or 14 cannot currently be used for such a global extrapolation. Here, we apply Equation 12 to extrapolate the spatial distributions of benthic OM reactivity from the global DOU distribution provided by Seiter et al. (2005a, 2005b), see Figure 9b) and Jørgensen et al. (2022, see Figure 9a). Importantly, the Log-transformed distribution of parameter a is back-converted to a linear scale (untransformed) using a correction factor (=2.48; based on the variance of log(a)) according to Middelburg et al. (1997) to counteract the systematic bias due to skewness in the log-transformed data.

The resulting global reactivity maps (Figure 9) reveal pronounced differences that can be explained by the assumptions underlying the two different DOU estimates. The global DOU estimates proposed by Jørgensen et al. (2022) cover the shallow coastal to the deep ocean and reveal a strong trend with SFD. DOU rates from Jørgensen et al. (2022) generally fall into the higher range of observed DOU rates ($[2.7 \cdot 10^{-1} - 4.9 \cdot 10^{1}]$ mmol m^{-2} d^{-1}). In contrast, the global DOU estimates proposed by Seiter et al. (2005a, 2005b) only cover water depths >1,000 m, are more heterogenous, and exhibit a wider DOU range compared to those in Jørgensen et al. (2022). As a result, OM reactivities based on the Jørgensen et al. (2022) DOU estimates (Figure 9a) do not only fall within a narrow range toward the higher end of the plausible reactivity spectrum ($k = [0.0012 - 0.1]$ year^{-1}; $a = [1.2 - 145.5]$ years), but also reveal a strong decrease in apparent OM reactivity (i.e., an increase in parameter a) with SFD. In contrast, the global distribution of OM reactivities derived on the basis of the Seiter et al. (2005a, 2005b) DOU estimates (Figure 9b) reveal a pronounced regional reactivity pattern and predict a wider range of OM reactivities ($k = [5 \cdot 10^{-4} - 0.009]$ year^{-1}; $a = [1.5 - 268]$ years). High OM reactivities (i.e., low a values) are predicted for sediments in the Arabian Sea, the Eastern Equatorial Pacific and the upwelling areas associated with eastern boundary currents on continental margins, while the large open ocean basins display a heterogeneous pattern with low apparent OM reactivities (i.e., high a values) in the central regions and higher apparent OM reactivity in the vicinity of the margins/continental slopes. This emerging global reactivity pattern is in good agreement with the local and regional reactivity results discussed earlier. Disagreements between site-specific inversely determined OM reactivities (see the previous section) and globally extrapolated apparent OM reactivities for deeper sediments arise for two main reasons: (a) underestimating/overestimating OM reactivity for very low/high OM

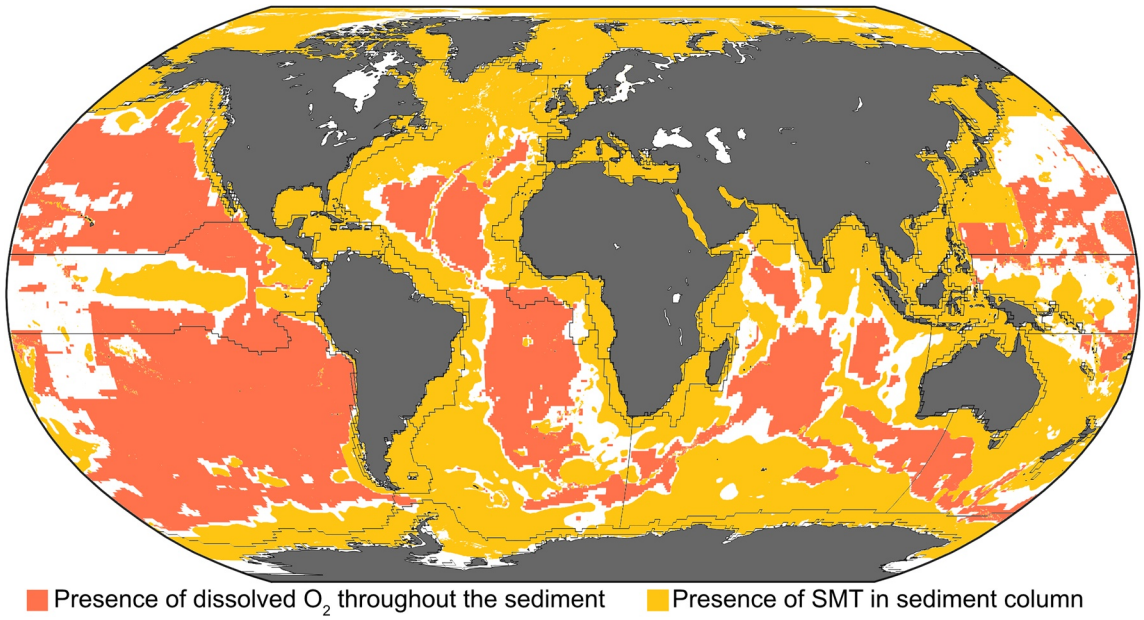

Figure 10. Potential proxies for organic matter (OM) reactivity in marine sediments using the sulfate-methane transition zone (SMTZ) and the penetration depth of O_2. In the yellow areas the SMTZ is present in the sediment down to a depth of 1,000 m (data from Egger et al. (2018)), which is indicative of mid to high OM reactivities. In the orange areas dissolved O_2 penetrates throughout the sediment to the underlying oceanic basement (data from LaRowe et al. (2020)) which is indicative of low to very low OM reactivities.

contents as a consequence of neglecting the influence of OM content, and (b) a bias in data or poor data coverage in certain areas (e.g., the South Pacific and Atlantic, Indian Ocean, Southern Ocean, as well as the shelf and the continental slope environments). However, deviations between site-specific, inversely determined OM reactivities and the predicted global OM reactivity map are generally smaller than one order of magnitude.

A notable exception are the large "biogeochemical" deserts in the central ocean gyres. These areas are under sampled and thus underrepresented in global data sets. The global DOU estimate by Seiter et al. (2005a, 2005b) reports DOU rates of [1.44–2] mmol m^{-2} d^{-1} for the central South Pacific, while recent observational data from the South Pacific (D'Hondt et al., 2015; Fischer et al., 2009; Røy et al., 2012) indicate that DOU rates, and thus OM reactivities, are likely several orders of magnitude lower ($2.3 \cdot 10^{-4}$ mmol m^{-2} d^{-1}). The estimated spatial distribution of deep OPDs (D'Hondt et al., 2015) and SMTZ (Egger et al., 2018) provide a first clue of the maximum spatial extend of the area for which OM reactivities are likely overpredicted (i.e., orange area, Figure 10).

In summary, the global distribution of OM reactivities derived based on the DOU estimates proposed by Jørgensen et al. (2022) captures the high OM reactivities that are often observed in the coastal ocean, but overpredicts OM reactivity in the large open ocean basins and does not resolve regional differences in OM reactivity. On the other hand, the global distribution of OM reactivities based on DOU estimates proposed by Seiter et al. (2005a, 2005b) does not cover coastal sediments, but resolves emerging regional patterns in open ocean. We thus advise to use the global prediction of OM reactivity based on the Seiter et al. (2005a, 2005b) DOU data for deep sediments and based on Jørgensen et al. (2022) for coastal sediments while being conscious of the disagreements that arise due to data bias and the lack of independent global data sets.

4. Conclusion

In summary, the comparison of simulation results with local and global observational data reveals that our inversely determined a-parameters (i.e., apparent OM reactivity) capture local and global patterns in observed benthic oxygen dynamics well and thus increases the confidence in the robustness of our inverse modeling results.

We inversely determine the apparent reactivity of OM in marine sediments (i.e., the RCM parameter a and ν) from a global data set of 355 observed DOU rates that vary over orders of magnitude, ranging from high ($k = 0.25$ $year^{-1}$; $a = 0.6$ years in the South Polar region) to extremely low ($k = 6.3 \cdot 10^{-8}$ $year^{-1}$;

$a = 5.6 \cdot 10^6$ years in the oligotrophic, central South Pacific) apparent OM reactivities in ocean sediments. These findings highlight the high intra- and inter-regional heterogeneity in apparent benthic OM reactivity, but also reveal clear regional patterns that broadly agree with observations and prior assessments. The emerging patterns in benthic OM reactivity can be directly linked back to environmental and ecological characteristics of the respective depositional environments, thus providing important insights into the environmental factors that control OM reactivity, and highlighting regions where in-depth future measurements are warranted.

The highest apparent OM reactivities are found in the Arabian Sea, South Polar region, Subpolar and the Eastern Equatorial Pacific, and individual sites in Eastern Boundary Systems, the Western Equatorial Pacific, the Greenland provinces, and at sites underlying the Polar Front in the Indian Ocean province. They can be linked back to environmental conditions that limited pelagic OM degradation through accelerated vertical (phytodetrital aggregates, mineral ballast, fronts, mesoscale eddies and ice edge effects) or lateral (gravity-driven mass flow) transport of OM to the sediment or by factors that directly limit pelagic degradation (e.g., presence of OMZ, low temperature). As a consequence, reactive OM compounds reach the sediment, where they support intense microbial activity and trigger rapid oxygen consumption. The lowest apparent OM reactivities for deep-sea sediments underlying the oligotrophic, central ocean gyres. Here, extremely low rates of surface ocean primary production, remoteness from continental margins, low sinking velocities of small OM particles, and deep water columns limit the flux and the quality of OM arriving at the sea floor. Contrary to the traditional view that sedimentary OM reactivity decreases with water depth, our results indicate that not all deep-sea sediments are characterized by a low apparent OM reactivity. For instance, we estimate comparably high apparent OM reactivities for the Atlantic Ocean and continental slope and deep-sea sediments close to productive continental margins. Here, comparably reactive OM is laterally transported from the productive margins to the slope or deep ocean sediment. Furthermore, regions that are characterized by high turbulent kinetic eddy dispersion, such as western boundary systems or the southern Argentine margin, also receive comparably reactive OM from distal regions. Inverse model results reveal a heterogeneous distribution of apparent OM reactivities (i.e., $k = \nu/a$) in most other provinces. Here, OM that is derived from diverse sources is distributed across the regions by a complex interplay of hydrodynamic processes, including sediment resuspension and lateral transport. Our results thus highlight the need for a better mechanistic understanding of the environmental controls on apparent OM reactivity (i.e., $k = \nu/a$).

Finally, inverse model results reveal a clear link between apparent OM reactivity (i.e., $k = \nu/a$), DOU rates and, to a lesser extent, surface sediment OM content and SFD. Based on the data from the 355 investigated individual sites, we derive a set of empirical relationships that link benthic OM reactivity (i.e., $k = \nu/a$) with DOU, surface sediment OM content and SFD. We then use the transfer functions to derive the first global maps of benthic OM reactivity based on gridded global DOU data sets. Despite the observational bias inherent in these data sets, the global maps provide a good first-order estimate of the apparent benthic OM reactivity that agrees with our current mechanistic understanding and observations.

Conflict of Interest

The authors declare no conflicts of interest relevant to this study.

Data Availability Statement

All data used in the inverse model study has been taken from the published sources referenced in the text (Sections 2.1 and 2.3). The global TOC and DOU data sets published in Seiter et al. (2005a, 2005b) and Seiter et al. (2004) data set available here: Seiter et al. (2005a, 2005b), while the published DOU data set published by Jørgensen et al. (2022) available here (Egger et al., 2022). Data for the bottom water boundary conditions are from NOAA World Ocean Atlas 2016 (Lauvset et al., 2016). These data were used as boundary conditions for the model and the DOU rates were inversely fitted in writing this manuscript. The source code of OMEN-SED-RCM is available as a supplementary material to Pika et al. (2021) and see Pika and Hülse (2021) and is also found on Github at https://github.com/PhilipPika/OMEN-SED. The data underlying Figure 9 are available as supplementary information here: https://doi.org/10.5281/zenodo.8107762 and see Pika (2023). Figures were made with Matlab version 9.13, under the academic license available at Mathworks: https://mathworks.com.

Acknowledgments
SA and PP were supported by funding from the European Union's Horizon 2020 research and innovation programme under the Marie Skłodowska-Curie grant agreement no. 643052 (C-CASCADES). DH is supported by a postdoctoral fellowship from the Simons Foundation (Award ID 653829).

References

Alldredge, A. L., Gotschalk, C., Passow, U., & Riebesell, U. (1995). Mass aggregation of diatom blooms: Insights from a mesocosm study. *Deep Sea Research Part II: Topical Studies in Oceanography*, *42*(1), 9–27. https://doi.org/10.1016/0967-0645(95)00002-8

Aller, R. C. (1990). Bioturbation and manganese cycling in hemipelagic sediments. *Philosophical Transactions of the Royal Society A: Mathematical, Physical & Engineering Sciences*, *331*(1616), 51–68. https://doi.org/10.1098/rsta.1990.0056

Aller, R. C., & Blair, N. E. (2006). Carbon remineralization in the Amazon-Guianas tropical mobile mudbelt: A sedimentary incinerator. *Continental Shelf Research*, *26*(17–18), 2241–2259. https://doi.org/10.1016/j.csr.2006.07.016

Aller, R. C., & Cochran, J. K. (2019). The critical role of bioturbation for particle dynamics, priming potential, and organic C remineralization in marine sediments: Local and basin scales. *Frontiers in Earth Science*, *7*. https://doi.org/10.3389/feart.2019.00157

Anderson, L. A., & Sarmiento, J. L. (1994). Redfield ratios of remineralization determined by nutrient data analysis. *Global Biogeochemical Cycles*, *8*(1), 65–80. https://doi.org/10.1029/93GB03318

Andersson, J. H., Wijsman, J. W., Herman, P. M., Middleburg, J. J., Soetaert, K., & Heip, C. (2004). Respiration patterns in the deep ocean. *Geophysical Research Letters*, *31*(3), 1–4. https://doi.org/10.1029/2003GL018756

Antia, A. N., Koeve, W., Fischer, G., Blanz, T., Schulz-Bull, D., Schölten, J., et al. (2001). Basin-wide particulate carbon flux in the Atlantic Ocean: Regional export patterns and potential for atmospheric CO_2 sequestration. *Global Biogeochemical Cycles*, *15*(4), 845–862. https://doi.org/10.1029/2000GB001376

Archer, D., & Devol, A. (1992). Benthic oxygen fluxes on the Washington shelf and slope: A comparison of in situ microelectrode and chamber flux measurements. *Limnology & Oceanography*, *37*(3), 614–629. https://doi.org/10.4319/lo.1992.37.3.0614

Arnarson, T. S., & Keil, R. G. (2007). Changes in organic matter–mineral interactions for marine sediments with varying oxygen exposure times. *Geochimica et Cosmochimica Acta*, *71*(14), 3545–3556. https://doi.org/10.1016/j.gca.2007.04.027

Arndt, S., Hetzel, A., & Brumsack, H. J. (2009). Evolution of organic matter degradation in Cretaceous black shales inferred from authigenic barite: A reaction-transport model. *Geochimica et Cosmochimica Acta*, *73*(7), 2000–2022. https://doi.org/10.1016/j.gca.2009.01.018

Arndt, S., Jørgensen, B. B., LaRowe, D. E., Middelburg, J. J., Pancost, R. D., & Regnier, P. (2013). Quantifying the degradation of organic matter in marine sediments: A review and synthesis. *Earth-Science Reviews*, *123*, 53–86. https://doi.org/10.1016/j.earscirev.2013.02.008

Arnosti, C. (2008). Functional differences between Arctic seawater and sedimentary microbial communities: Contrasts in microbial hydrolysis of complex substrates. *FEMS Microbiology Ecology*, *66*(2), 343–351. https://doi.org/10.1111/j.1574-6941.2008.00587.x

Arnosti, C. (2015). Contrasting patterns of peptidase activities in seawater and sediments: An example from arctic fjords of Svalbard. *Marine Chemistry*, *168*, 151–156. https://doi.org/10.1016/j.marchem.2014.09.019

Arnosti, C., & Holmer, M. (2003). Carbon cycling in a continental margin sediment: Contrasts between organic matter characteristics and remineralization rates and pathways. *Estuarine, Coastal and Shelf Science*, *58*(1), 197–208. https://doi.org/10.1016/S0272-7714(03)00077-5

Arnosti, C., Jørgensen, B., Sagemann, J., & Thamdrup, B. (1998). Temperature dependence of microbial degradation of organic matter in marine sediments: Polysaccharide hydrolysis, oxygen consumption, and sulfate reduction. *Marine Ecology Progress Series*, *165*, 59–70. https://doi.org/10.3354/meps165059

Arnosti, C., Steen, A. D., Ziervogel, K., Ghobrial, S., & Jeffrey, W. H. (2011). Latitudinal gradients in degradation of marine dissolved organic carbon. *PLoS One*, *6*(12), e28900. https://doi.org/10.1371/journal.pone.0028900

Atwood, T. B., Witt, A., Mayorga, J., Hammill, E., & Sala, E. (2020). Global patterns in marine sediment carbon stocks. *Frontiers in Marine Science*, *7*. https://doi.org/10.3389/fmars.2020.00165

Babonneau, N., Savoye, B., Cremer, M., & Klein, B. (2002). Morphology and architecture of the present canyon and channel system of the Zaire deep-sea fan. *Marine and Petroleum Geology*, *19*(4), 445–467. https://doi.org/10.1016/S0264-8172(02)00009-0

Bao, R., van der Voort, T. S., Zhao, M., Guo, X., Montluçon, D. B., McIntyre, C., & Eglinton, T. I. (2018). Influence of hydrodynamic processes on the fate of sedimentary organic matter on continental margins. *Global Biogeochemical Cycles*, *32*(9), 1420–1432. https://doi.org/10.1029/2018GB005921

Beaulieu, C., Henson, S. A., Sarmiento, J. L., Dunne, J. P., Doney, S. C., Rykaczewski, R. R., & Bopp, L. (2013). Factors challenging our ability to detect long-term trends in ocean chlorophyll. *Biogeosciences*, *10*(4), 2711–2724. https://doi.org/10.5194/bg-10-2711-2013

Benthien, A., & Müller, P. J. (2000). Anomalously low alkenone temperatures caused by lateral particle and sediment transport in the Malvinas Current region, western Argentine Basin. *Deep-Sea Research Part I Oceanographic Research Papers*, *47*(12), 2369–2393. https://doi.org/10.1016/S0967-0637(00)00030-3

Berner, R. A. (1980a). *Early diagenesis: A theoretical approach*. Princeton University Press.

Berner, R. A. (1980b). A rate model for organic matter decomposition during bacterial sulfate reduction in marine sediments. In *Biogéochimie de la matière organique à l'interface eau-sédiment marin* (Vol. 293, pp. 35–44). Centre National de la Recherche Scientifique.

Berner, R. A. (1990). Atmospheric carbon dioxide levels over phanerozoic time. *Science*, *249*(4975), 1382–1386. https://doi.org/10.1126/science.249.4975.1382

Bianchi, T. S., Cui, X., Blair, N. E., Burdige, D. J., Eglinton, T. I., & Galy, V. (2018). Centers of organic carbon burial and oxidation at the land-ocean interface. *Organic Geochemistry*, *115*, 138–155. https://doi.org/10.1016/j.orggeochem.2017.09.008

Black, K. S., Fones, G. R., Peppe, O. C., Kennedy, H. A., & Bentaleb, I. (2001). An autonomous benthic lander. *Continental Shelf Research*, *21*(8–10), 859–877. https://doi.org/10.1016/S0278-4343(00)00116-3

Blair, N. E., & Aller, R. C. (2012). The fate of terrestrial organic carbon in the marine environment. *Annual Review of Marine Science*, *4*(1), 401–423. https://doi.org/10.1146/annurev-marine-120709-142717

Boetius, A., & Damm, E. (1998). Benthic oxygen uptake, hydrolytic potentials and microbial biomass at the Arctic continental slope. *Deep-Sea Research Part I Oceanographic Research Papers*, *45*(2–3), 239–275. https://doi.org/10.1016/S0967-0637(97)00052-6

Boetius, A., Ferdelman, T., & Lochte, K. (2000). Bacterial activity in sediments of the deep Arabian Sea in relation to vertical flux. *Deep-Sea Research Part II Topical Studies in Oceanography*, *47*(14), 2835–2875. https://doi.org/10.1016/S0967-0645(00)00051-5

Boetius, A., Springer, B., & Petry, C. (2000). Microbial activity and particulate matter in the benthic nepheloid layer (BNL) of the deep Arabian Sea. *Deep-Sea Research Part II Topical Studies in Oceanography*, *47*(14), 2687–2706. https://doi.org/10.1016/S0967-0645(00)00045-X

Boudreau, B. P. (1997). *Diagenetic models and their implementation* (Vol. 505). Springer Berlin.

Boudreau, B. P., Arnosti, C., Jørgensen, B. B., & Canfield, D. E. (2008). Comment on "Physical model for the decay and preservation of marine organic carbon". *Science*, *319*(5870), 1616b. https://doi.org/10.1126/science.1148589

Boudreau, B. P., & Canfield, D. E. (1993). A comparison of closed- and open-system models for porewater pH and calcite-saturation state. *Geochimica et Cosmochimica Acta*, *57*(2), 317–334. https://doi.org/10.1016/0016-7037(93)90434-X

Boudreau, B. P., & Ruddick, B. R. (1991). On a reactive continuum representation of organic matter diagenesis. *American Journal of Science*, *291*(5), 507–538. https://doi.org/10.2475/ajs.291.5.507

Bourgeois, S., Archambault, P., & Witte, U. (2017). Organic matter remineralization in marine sediments: A pan-Arctic synthesis. *Global Biogeochemical Cycles*, *31*(1), 190–213. https://doi.org/10.1002/2016GB005378

Bröder, L., Tesi, T., Andersson, A., Semiletov, I., & Gustafsson, Ö. (2018). Bounding cross-shelf transport time and degradation in Siberian-Arctic land-ocean carbon transfer. *Nature Communications*, *9*(1), 806. https://doi.org/10.1038/s41467-018-03192-1

Burdige, D. J. (2007). Preservation of organic matter in marine sediments: Controls, mechanisms, and an imbalance in sediment organic carbon budgets? *Chemical Reviews*, *107*(2), 467–485. https://doi.org/10.1021/cr050347q

Burwicz, E., Rüpke, L., & Wallmann, K. (2011). Estimation of the global amount of submarine gas hydrates formed via microbial methane formation based on numerical reaction-transport modeling and a novel parameterization of Holocene sedimentation. *Geochimica et Cosmochimica Acta*, *75*(16), 4562–4576. https://doi.org/10.1016/j.gca.2011.05.029

Canfield, D. (1994). Factors influencing organic carbon preservation in marine sediments. *Chemical Geology*, *114*(3–4), 315–329. https://doi.org/10.1016/0009-2541(94)90061-2

Canfield, D., Jørgensen, B., Fossing, H., Glud, R., Gundersen, J., Ramsing, N., et al. (1993). Pathways of organic carbon oxidation in three continental margin sediments. *Marine Geology*, *113*(1–2), 27–40. https://doi.org/10.1016/0025-3227(93)90147-N

Canuel, E. A., & Martens, C. S. (1996). Reactivity of recently deposited organic matter: Degradation of lipid compounds near the sediment-water interface. *Geochimica et Cosmochimica Acta*, *60*(10), 1793–1806. https://doi.org/10.1016/0016-7037(96)00045-2

Cho, B. C., & Azam, F. (1988). Major role of bacteria in biogeochemical fluxes in the Ocean's interior. *Nature*, *332*(6163), 441–443. https://doi.org/10.1038/332441a0

Cowie, G. L., Hedges, J. I., & Calvert, S. E. (1992). Sources and relative reactivities of amino acids, neutral sugars, and lignin in an intermittently anoxic marine environment. *Geochimica et Cosmochimica Acta*, *56*(5), 1963–1978. https://doi.org/10.1016/0016-7037(92)90323-B

Dauwe, B., Middelburg, J. J., Herman, P. M. J., & Heip, C. H. R. (1999). Linking diagenetic alteration of amino acids and bulk organic matter reactivity. *Limnology & Oceanography*, *44*(7), 1809–1814. https://doi.org/10.4319/lo.1999.44.7.1809

Devol, A. H., & Hartnett, H. E. (2001). Role of the oxygen-deficient zone in transfer of organic carbon to the deep ocean. *Limnology & Oceanography*, *46*(7), 1684–1690. https://doi.org/10.4319/lo.2001.46.7.1684

DeVries, T., & Weber, T. (2017). The export and fate of organic matter in the ocean: New constraints from combining satellite and oceanographic tracer observations. *Global Biogeochemical Cycles*, *31*(3), 535–555. https://doi.org/10.1002/2016GB005551

D'Hondt, S., Inagaki, F., Zarikian, C. A., Abrams, L. J., Dubois, N., Engelhardt, T., et al. (2015). Presence of oxygen and aerobic communities from sea floor to basement in deep-sea sediments. *Nature Geoscience*, *8*(4), 299–304. https://doi.org/10.1038/ngeo2387

D'Hondt, S., Spivack, A. J., Pockalny, R., Ferdelman, T. G., Fischer, J. P., Kallmeyer, J., et al. (2009). Subseafloor sedimentary life in the South Pacific Gyre. *Proceedings of the National Academy of Sciences of the United States of America*, *106*(28), 11651–11656. https://doi.org/10.1073/pnas.0811793106

Dickson, R. R., & McCave, I. N. (1986). Nepheloid layers on the continental slope west of Porcupine Bank. *Deep-Sea Research, Part A: Oceanographic Research Papers*, *33*(6), 791–818. https://doi.org/10.1016/0198-0149(86)90089-0

Egger, M., Jørgensen, B. B., Wenzhöfer, F., & Glud, R. N. (2022). Global seabed oxygen uptake (Jorgensen et al., 2022) [Dataset]. https://doi.org/10.6084/m9.figshare.19432982.v1

Egger, M., Riedinger, N., Mogollón, J. M., & Jørgensen, B. B. (2018). Global diffusive fluxes of methane in marine sediments. *Nature Geoscience*, *11*(6), 421–425. https://doi.org/10.1038/s41561-018-0122-8

Emerson, S., Fischer, K., Reimers, C., & Heggie, D. (1985). Organic carbon dynamics and preservation in deep-sea sediments. *Deep-Sea Research, Part A: Oceanographic Research Papers*, *32*(1), 1–21. https://doi.org/10.1016/0198-0149(85)90014-7

Emerson, S., & Hedges, J. I. (2003). Sediment diagenesis and benthic flux. In *Treatise on geochemistry* (Vol. 6–9, pp. 293–319). Elsevier. https://doi.org/10.1016/B0-08-043751-6/06112-0

Fabiano, M., & Danovaro, R. (1998). Enzymatic activity, bacterial distribution, and organic matter composition in sediments of the Ross Sea (Antarctica). *Applied and Environmental Microbiology*, *64*(10), 3838–3845. https://doi.org/10.1128/aem.64.10.3838-3845.1998

Fabiano, M., Danovaro, R., Chiantore, M., & Pusceddu, A. (2000). Bacteria, Protozoa and organic matter composition in the sediments of Terra Nova Bay (Ross Sea). In *Ross sea ecology* (pp. 159–169). Springer Berlin Heidelberg. https://doi.org/10.1007/978-3-642-59607-0_13

Fischer, J. P., Ferdelman, T. G., D'Hondt, S., Røy, H., & Wenzhöfer, F. (2009). Oxygen penetration deep into the sediment of the South Pacific gyre. *Biogeosciences*, *6*(8), 1467–1478. https://doi.org/10.5194/bg-6-1467-2009

Freitas, F. S., Pika, P. A., Kasten, S., Jørgensen, B. B., Rassmann, J., Rabouille, C., et al. (2021). New insights into large-scale trends of apparent organic matter reactivity in marine sediments and patterns of benthic carbon transformation. *Biogeosciences*, *18*(15), 4651–4679. https://doi.org/10.5194/bg-18-4651-2021

Gerdes, D., Klages, M., Arntz, W. E., Herman, R. L., Galéron, J., & Hain, S. (1992). Quantitative investigations on macrobenthos communities of the southeastern Weddell Sea shelf based on multibox corer samples. *Polar Biology*, *12*(2), 291–301. https://doi.org/10.1007/BF00238272

Giordani, P., Helder, W., Koning, E., Miserocchi, S., Danovaro, R., & Malaguti, A. (2002). Gradients of benthic-pelagic coupling and carbon budgets in the Adriatic and northern Ionian Sea. *Journal of Marine Systems*, *33–34*, 365–387. https://doi.org/10.1016/S0924-7963(02)00067-2

Glud, R. N. (2008). Oxygen dynamics of marine sediments. *Marine Biology Research*, *4*(4), 243–289. https://doi.org/10.1080/17451000801888726

Glud, R. N., Gundersen, J., & Holby, O. (1999). Benthic in situ respiration in the upwelling area off central Chile. *Marine Ecology Progress Series*, *186*, 9–18. https://doi.org/10.3354/meps186009

Glud, R. N., Gundersen, J. K., Barker Jørgensen, B., Revsbech, N. P., & Schulz, H. D. (1994). Diffusive and total oxygen uptake of deep-sea sediments in the eastern South Atlantic Ocean: In situ and laboratory measurements. *Deep Sea Research Part I: Oceanographic Research Papers*, *41*(11–12), 1767–1788. https://doi.org/10.1016/0967-0637(94)90072-8

Glud, R. N., Gundersen, J. K., Røy, H., & Jørgensen, B. B. (2003). Seasonal dynamics of benthic O_2 uptake in a semienclosed bay: Importance of diffusion and faunal activity. *Limnology & Oceanography*, *48*(3), 1265–1276. https://doi.org/10.4319/lo.2003.48.3.1265

Glud, R. N., Holby, O., Hoffmann, F., & Canfield, D. (1998). Benthic mineralization and exchange in Arctic sediments (Svalbard, Norway). *Marine Ecology Progress Series*, *173*, 237–251. https://doi.org/10.3354/meps173237

Glud, R. N., Stahl, H., Berg, P., Wenzhöfer, F., Oguri, K., & Kitazato, H. (2009). In situ microscale variation in distribution and consumption of 2: A case study from a deep ocean margin sediment (Sagami Bay, Japan). *Limnology & Oceanography*, *54*(1), 1–12. https://doi.org/10.4319/lo.2009.54.1.0001

Graf, G. (1989). Benthic-pelagic coupling in a deep-sea benthic community. *Nature*, *341*(6241), 437–439. https://doi.org/10.1038/341437a0

Graf, G., Gerlach, S. A., Linke, P., Queisser, W., Ritzrau, W., Scheltz, A., et al. (1995). Benthic-pelagic coupling in the Greenland-Norwegian Sea and its effect on the geological record. *Geologische Rundschau*, *84*(1), 49–58. https://doi.org/10.1007/BF00192241

Grebmeier, J. M., Overland, J. E., Moore, S. E., Farley, E. V., Carmack, E. C., Cooper, L. W., et al. (2006). A major ecosystem shift in the northern Bering Sea. *Science*, *311*(5766), 1461–1464. https://doi.org/10.1126/science.1121365

Grossart, H. P., & Ploug, H. (2001). Microbial degradation of organic carbon and nitrogen on diatom aggregates. *Limnology & Oceanography*, *46*(2), 267–277. https://doi.org/10.4319/lo.2001.46.2.0267

Hales, B., & Emerson, S. (1996). In situ electrode measurements. *Global Biogeochemical Cycles*, *10*(3), 527–541. https://doi.org/10.1029/96gb01522

Hantschel, T., & Kauerauf, A. I. (2009). *Fundamentals of basin and petroleum systems modeling*. Springer Berlin Heidelberg. https://doi.org/10.1007/978-3-540-72318-9

Harada, N. (2016). Review: Potential catastrophic reduction of sea ice in the western Arctic Ocean: Its impact on biogeochemical cycles and marine ecosystems. *Global and Planetary Change*, *136*, 1–17. https://doi.org/10.1016/j.gloplacha.2015.11.005

Hartnett, H., Keil, G. R., Hedges, I. J., & Devol, H. A. (1998). Influence of oxygen exposure time on organic carbon preservation in continental margin sediments. *Nature*, *391*, 572–574. https://doi.org/10.1038/35351

Hartnett, H. E., & Seitzinger, S. P. (2003). High-resolution nitrogen gas profiles in sediment porewaters using a new membrane probe for membrane-inlet mass spectrometry. *Marine Chemistry*, *83*(1–2), 23–30. https://doi.org/10.1016/S0304-4203(03)00093-8

Head, I. M., Jones, D. M., & Röling, W. F. M. (2006). Marine microorganisms make a meal of oil. *Nature Reviews Microbiology*, *4*(3), 173–182. https://doi.org/10.1038/nrmicro1348

Hedges, J. I., Hu, F. S., Devol, A. H., Hartnett, H. E., Tsamakis, E., & Keil, R. G. (1999). Sedimentary organic matter preservation; a test for selective degradation under oxic conditions. *American Journal of Science*, *299*(7–9), 529–555. https://doi.org/10.2475/ajs.299.7-9.529

Hedges, J. I., & Keil, R. G. (1995). Sedimentary organic matter preservation: An assessment and speculative synthesis. *Marine Chemistry*, *49*(2–3), 81–115. https://doi.org/10.1016/0304-4203(95)00008-F

Heezen, B. C., & Hollister, C. (1964). Deep-sea current evidence from abyssal sediments. *Marine Geology*, *1*(2), 141–174. https://doi.org/10.1016/0025-3227(64)90012-X

Hemingway, J. D., Rothman, D. H., Grant, K. E., Rosengard, S. Z., Eglinton, T. I., Derry, L. A., & Galy, V. V. (2019). Mineral protection regulates long-term global preservation of natural organic carbon. *Nature*, *570*(7760), 228–231. https://doi.org/10.1038/s41586-019-1280-6

Hensen, C., Landenberger, H., Zabel, M., & Schulz, H. D. (1998). Quantification of diffusive benthic fluxes of nitrate, phosphate, and silicate in the southern Atlantic Ocean. *Global Biogeochemical Cycles*, *12*(1), 193–210. https://doi.org/10.1029/97GB02731

Hensen, C., Zabel, M., & Schulz, H. D. (2000). A comparison of benthic nutrient fluxes from deep-sea sediments off Namibia and Argentina. *Deep-Sea Research Part II Topical Studies in Oceanography*, *47*(9–11), 2029–2050. https://doi.org/10.1016/S0967-0645(00)00015-1

Hoefs, M. J., Rijpstra, W. C., & Sinninghe Damsté, J. S. (2002). The influence of oxic degradation on the sedimentary biomarker record I: Evidence from Madeira Abyssal Plain turbidites. *Geochimica et Cosmochimica Acta*, *66*(15), 2719–2735. https://doi.org/10.1016/S0016-7037(02)00864-5

Hollister, C. D., & McCave, I. N. (1984). Sedimentation under deep-sea storms. *Nature*, *309*(5965), 220–225. https://doi.org/10.1038/309220a0

Honjo, S., Dymond, J., Prell, W., & Ittekkot, V. (1999). Monsoon-controlled export fluxes to the interior of the Arabian Sea. *Deep Sea Research Part II: Topical Studies in Oceanography*, *46*(8), 1859–1902. https://doi.org/10.1016/S0967-0645(99)00047-8

Hülse, D., Arndt, S., Daines, S., Regnier, P., & Ridgwell, A. (2018). OMEN-SED 1.0: A novel, numerically efficient organic matter sediment diagenesis module for coupling to Earth system models. *Geoscientific Model Development*, *11*(7), 2649–2689. https://doi.org/10.5194/gmd-11-2649-2018

Hulthe, G., Hulth, S., & Hall, P. O. J. (1998). Effect of oxygen on degradation rate of refractory and labile organic matter in continental margin sediments—A comparative survey of certain organic and inorganic compounds in an oxic and anoxic Baltic basin. *Geochimica et Cosmochimica Acta*, *62*(8), 1319–1328. https://doi.org/10.1016/S0016-7037(98)00044-1

Inthorn, M., Mohrholz, V., & Zabel, M. (2006). Nepheloid layer distribution in the Benguela upwelling area offshore Namibia. *Deep Sea Research Part I: Oceanographic Research Papers*, *53*(8), 1423–1438. https://doi.org/10.1016/j.dsr.2006.06.004

Iversen, M. H., & Ploug, H. (2013). Temperature effects on carbon-specific respiration rate and sinking velocity of diatom aggregates–potential implications for deep ocean export processes. *Biogeosciences*, *10*(6), 4073–4085. https://doi.org/10.5194/bg-10-4073-2013

Jahnke, R. A. (1996). The global ocean flux of particulate organic carbon: Areal distribution and magnitude. *Global Biogeochemical Cycles*, *10*(1), 71–88. https://doi.org/10.1029/95GB03525

Jahnke, R. A., Emerson, S., Reimers, C., Schuffert, J., Ruttenberg, K., & Archer, D. (1989). Benthic recycling of biogenic debris in the eastern tropical Atlantic Ocean. *Geochimica et Cosmochimica Acta*, *53*(11), 2947–2960. https://doi.org/10.1016/0016-7037(89)90171-3

Jørgensen, B. B., & Kasten, S. (2006). Sulfur cycling and methane oxidation. In *Marine geochemistry* (pp. 271–309). Springer-Verlag. https://doi.org/10.1007/3-540-32144-6_8

Jørgensen, B. B., & Revsbech, N. P. (1985). Diffusive boundary layers and the oxygen uptake of sediments and detritus. *Limnology & Oceanography*, *30*(1), 111–122. https://doi.org/10.4319/lo.1985.30.1.0111

Jørgensen, B. B., Wenzhöfer, F., Egger, M., & Glud, R. N. (2022). Sediment oxygen consumption: Role in the global marine carbon cycle. *Earth-Science Reviews*, *228*, 103987. https://doi.org/10.1016/j.earscirev.2022.103987

Kadko, D. C., Washburn, L., & Jones, B. (1991). Evidence of subduction within cold filaments of the northern California Coastal Transition Zone. *Journal of Geophysical Research*, *96*(C8), 14909. https://doi.org/10.1029/91jc00885

Kantor, B., Zehavi, S., & Salzman, J. (1992). Phase-shifted surface-acoustic-wave resonator. *IEEE Transactions on Ultrasonics, Ferroelectrics, and Frequency Control*, *39*(3), 319–323. https://doi.org/10.1109/58.143164

Keil, R. G., Dickens, A. F., Arnarson, T., Nunn, B. L., & Devol, A. H. (2004). What is the oxygen exposure time of laterally transported organic matter along the Washington margin? *Marine Chemistry*, *92*(1–4), 157–165. https://doi.org/10.1016/j.marchem.2004.06.024

Keil, R. G., Montluçon, D. B., Prahl, F. G., & Hedges, J. I. (1994). Sorptive preservation of labile organic matter in marine sediments. *Nature*, *370*(6490), 549–552. https://doi.org/10.1038/370549a0

Keil, R. G., Neibauer, J. A., Biladeau, C., Van Der Elst, K., & Devol, A. H. (2016). A multiproxy approach to understanding the "enhanced" flux of organic matter through the oxygen-deficient waters of the Arabian Sea. *Biogeosciences*, *13*(7), 2077–2092. https://doi.org/10.5194/bg-13-2077-2016

Kim, J. S., Kug, J. S., Jeong, S. J., Park, H., & Schaepman-Strub, G. (2020). Extensive fires in southeastern Siberian permafrost linked to preceding Arctic Oscillation. *Science Advances*, *6*(2), 1–8. https://doi.org/10.1126/sciadv.aax3308

Knoblauch, C., Jørgensen, B. B., & Harder, J. (1999). Community size and metabolic rates of psychrophilic sulfate-reducing bacteria in arctic marine sediments. *Applied and Environmental Microbiology*, *65*(9), 4230–4233. https://doi.org/10.1128/aem.65.9.4230-4233.1999

Koho, K. A., Nierop, K. G., Moodley, L., Middelburg, J. J., Pozzato, L., Soetaert, K., et al. (2013). Microbial bioavailability regulates organic matter preservation in marine sediments. *Biogeosciences*, *10*(2), 1131–1141. https://doi.org/10.5194/bg-10-1131-2013

Kristensen, E., & Holmer, M. (2001). Decomposition of plant materials in marine sediment exposed to different electron acceptors (O_2, $NO_3^-$and SO_4^{2-}), with emphasis on substrate origin, degradation kinetics, and the role of bioturbation. *Geochimica et Cosmochimica Acta*, *65*(3), 419–433. https://doi.org/10.1016/S0016-7037(00)00532-9

Lalonde, K., Mucci, A., Ouellet, A., & Gélinas, Y. (2012). Preservation of organic matter in sediments promoted by iron. *Nature*, *483*(7388), 198–200. https://doi.org/10.1038/nature10855

Lampitt, R. S., & Antia, A. N. (1997). Particle flux in deep seas: Regional characteristics and temporal variability. *Deep-Sea Research Part I Oceanographic Research Papers*, *44*(8), 1377–1403. https://doi.org/10.1016/S0967-0637(97)00020-4

Lansard, B., Rabouille, C., Denis, L., & Grenz, C. (2008). In situ oxygen uptake rates by coastal sediments under the influence of the Rhône River (NW Mediterranean Sea). *Continental Shelf Research*, *28*(12), 1501–1510. https://doi.org/10.1016/j.csr.2007.10.010

Lansard, B., Rabouille, C., Denis, L., & Grenz, C. (2009). Benthic remineralization at the land-ocean interface: A case study of the Rhône River (NW Mediterranean Sea). *Estuarine, Coastal and Shelf Science*, *81*(4), 544–554. https://doi.org/10.1016/j.ecss.2008.11.025

LaRowe, D. E., Arndt, S., Bradley, J. A., Estes, E. R., Hoarfrost, A., Lang, S. Q., et al. (2020). The fate of organic carbon in marine sediments—New insights from recent data and analysis. *Earth-Science Reviews*, *204*, 103146. https://doi.org/10.1016/j.earscirev.2020.103146

LaRowe, D. E., Burwicz, E., Arndt, S., Dale, A. W., & Amend, J. P. (2017). Temperature and volume of global marine sediments. *Geology*, *45*(3), 275–278. https://doi.org/10.1130/G38601.1

LaRowe, D. E., & Van Cappellen, P. (2011). Degradation of natural organic matter: A thermodynamic analysis. *Geochimica et Cosmochimica Acta*, *75*(8), 2030–2042. https://doi.org/10.1016/j.gca.2011.01.020

Lauvset, S. K., Key, R. M., Olsen, A., van Heuven, S., Velo, A., Lin, X., et al. (2016). A new global interior ocean mapped climatology: The 1 x 1 GLODAP version 2. *Earth System Science Data*, *8*(2), 325–340. https://doi.org/10.5194/essd-8-325-2016

Lee, T. R., Wood, W. T., & Phrampus, B. J. (2019). A machine learning (kNN) approach to predicting global seafloor total organic carbon. *Global Biogeochemical Cycles*, *33*(1), 37–46. https://doi.org/10.1029/2018GB005992

Levin, L., & Gooday, A. (2003). The deep Atlantic Ocean. In *Ecosystems of the world* (pp. 160–198). Elsevier Science.

Lohse, L., Helder, W., Epping, E. H., & Balzer, W. (1998). Recycling of organic matter along a shelf-slope transect across the N.W. European continental margin (Goban Spur). *Progress in Oceanography*, *42*(1–4), 77–110. https://doi.org/10.1016/S0079-6611(98)00029-9

Longhurst, A., & Glen Harrison, W. (1988). Vertical nitrogen flux from the oceanic photic zone by diel migrant zooplankton and nekton. *Deep-Sea Research, Part A: Oceanographic Research Papers*, *35*(6), 881–889. https://doi.org/10.1016/0198-0149(88)90065-9

Longhurst, A., Sathyendranath, S., Platt, T., & Caverhill, C. (1995). An estimate of global primary production in the ocean from satellite radiometer data. *Journal of Plankton Research*, *17*(6), 1245–1271. https://doi.org/10.1093/plankt/17.6.1245

Luff, R., Wallmann, K., Grandel, S., & Schlüter, M. (2000). Numerical modeling of benthic processes in the deep Arabian Sea. *Deep Sea Research Part II: Topical Studies in Oceanography*, *47*(14), 3039–3072. https://doi.org/10.1016/S0967-0645(00)00058-8

Marcus, N. H., & Boero, F. (1998). Minireview: The importance of benthic-pelagic coupling and the forgotten role of life cycles in coastal aquatic systems. *Limnology & Oceanography*, *43*(5), 763–768. https://doi.org/10.4319/lo.1998.43.5.0763

Marquardt, M., Hensen, C., Pinero, E., Wallmann, K., & Haeckel, M. (2010). A transfer function for the prediction of gas hydrate inventories in marine sediments. *Biogeosciences*, *7*(9), 2925–2941. https://doi.org/10.5194/bg-7-2925-2010

Martin, W. R., & Bender, M. L. (1988). The variability of benthic fluxes and sedimentary remineralization rates in response to seasonally variable organic carbon rain rates in the deep sea: A modeling study. *American Journal of Science*, *288*(6), 561–574. https://doi.org/10.2475/ajs.288.6.561

Mayer, L. M. (1994). Relationships between mineral surfaces and organic carbon concentrations in soils and sediments. *Chemical Geology*, *114*(3–4), 347–363. https://doi.org/10.1016/0009-2541(94)90063-9

Mazuecos, I. P., Arístegui, J., Vázquez-Domínguez, E., Ortega-Retuerta, E., Gasol, J. M., & Reche, I. (2015). Temperature control of microbial respiration and growth efficiency in the mesopelagic zone of the South Atlantic and Indian oceans. *Deep Sea Research Part I: Oceanographic Research Papers*, *95*, 131–138. https://doi.org/10.1016/j.dsr.2014.10.014

McCave, I. N. (2019). *Nepheloid layers* (3rd ed.). Elsevier Ltd. https://doi.org/10.1016/B978-0-12-409548-9.11207-2

Middelburg, J. J. (1989). A simple rate model for organic matter decomposition in marine sediments. *Geochimica et Cosmochimica Acta*, *53*(7), 1577–1581. https://doi.org/10.1016/0016-7037(89)90239-1

Middelburg, J. J., Soetaert, K., & Herman, P. M. (1997). Empirical relationships for use in global diagenetic models. *Deep Sea Research Part I: Oceanographic Research Papers*, *44*(2), 327–344. https://doi.org/10.1016/S0967-0637(96)00101-X

Mollenhauer, G., Eglinton, T., Ohkouchi, N., Schneider, R., Müller, P., Grootes, P., & Rullkötter, J. (2003). Asynchronous alkenone and foraminifera records from the Benguela upwelling system. *Geochimica et Cosmochimica Acta*, *67*(12), 2157–2171. https://doi.org/10.1016/S0016-7037(03)00168-6

Mollenhauer, G., Inthorn, M., Vogt, T., Zabel, M., Sinninghe Damsté, J. S., & Eglinton, T. I. (2007). Aging of marine organic matter during cross-shelf lateral transport in the Benguela upwelling system revealed by compound-specific radiocarbon dating. *Geochemistry, Geophysics, Geosystems*, *8*(9), 1–16. https://doi.org/10.1029/2007GC001603

Mollenhauer, G., Kienast, M., Lamy, F., Meggers, H., Schneider, R. R., Hayes, J. M., & Eglinton, T. I. (2005). An evaluation of ^{14}C age relationships between co-occurring foraminifera, alkenones, and total organic carbon in continental margin sediments. *Paleoceanography*, *20*(1), 1–12. https://doi.org/10.1029/2004PA001103

Moodley, L., Nigam, R., Ingole, B., Prakash Babu, C., Panchang, R., Nanajkar, M., et al. (2011). Oxygen minimum seafloor ecological (mal) functioning. *Journal of Experimental Marine Biology and Ecology*, *398*(1–2), 91–100. https://doi.org/10.1016/j.jembe.2010.12.015

Murray, J. W., & Grundmanis, V. (1980). Oxygen consumption in pelagic marine sediments. *Science*, *209*(4464), 1527–1530. https://doi.org/10.1126/science.209.4464.1527

Murray, J. W., & Kuivila, K. M. (1990). Organic matter diagenesis in the northeast Pacific: Transition from aerobic red clay to suboxic hemipelagic sediments. *Deep Sea Research Part A. Oceanographic Research Papers*, *37*(1), 59–80. https://doi.org/10.1016/0198-0149(90)90029-U

Nedwell, D. B., Walker, T. R., Ellis-Evans, J. C., & Clarke, A. (1993). Measurements of seasonal rates and annual budgets of organic carbon fluxes in an Antarctic coastal environment at Signy Island, South Orkney Islands, suggest a broad balance between production and decomposition. *Applied and Environmental Microbiology*, *59*(12), 3989–3995. https://doi.org/10.1128/aem.59.12.3989-3995.1993

Ohkouchi, N., Eglinton, T. I., Keigwin, L. D., & Hayes, J. M. (2002). Spatial and temporal offsets between proxy records in a sediment drift. *Science*, *298*(5596), 1224–1227. https://doi.org/10.1126/science.1075287

Omand, M. M., D'Asaro, E. A., Lee, C. M., Perry, M. J., Briggs, N., Cetinić, I., & Mahadevan, A. (2015). Eddy-driven subduction exports particulate organic carbon from the spring bloom. *Science*, *348*(6231), 222–225. https://doi.org/10.1126/science.1260062

Orcutt, B. N., LaRowe, D. E., Biddle, J. F., Colwell, F. S., Glazer, B. T., Reese, B. K., et al. (2013). Microbial activity in the marine deep biosphere: Progress and prospects. *Frontiers in Microbiology*, *4*, 1–15. https://doi.org/10.3389/fmicb.2013.00189

Palanques, A., Isla, E., Puig, P., Sanchez-Cabeza, J. A., & Masqué, P. (2002). Annual evolution of downward particle fluxes in the Western Bransfield Strait (Antarctica) during the FRUELA project. *Deep Sea Research Part II: Topical Studies in Oceanography*, *49*(4–5), 903–920. https://doi.org/10.1016/S0967-0645(01)00130-8

Pfannkuche, O. (1993). Benthic response to the sedimentation of particulate organic matter at the BIOTRANS station, 47°N, 20°W. *Deep-Sea Research Part II*, *40*(1–2), 135–149. https://doi.org/10.1016/0967-0645(93)90010-K

Pfannkuche, O., & Lochte, K. (2000). The biogeochemistry of the deep Arabian Sea: Overview. *Deep-Sea Research Part II Topical Studies in Oceanography*, *47*(14), 2615–2628. https://doi.org/10.1016/S0967-0645(00)00041-2

Piepenburg, D., Schmid, M. K., & Gerdes, D. (2002). The benthos off King George Island (South Shetland Islands, Antarctica): Further evidence for a lack of a latitudinal biomass cline in the Southern Ocean. *Polar Biology*, *25*(2), 146–158. https://doi.org/10.1007/s003000100322

Pika, P. (2023). *Gridded global organic matter reactivity (RCM parameter a, in years)*. Zenodo. https://doi.org/10.5281/zenodo.8107762

Pika, P., & Hülse, D. (2021). PhilipPika/OMEN-SED-RCM-v1.1: Including plot functions [Software]. Zenodo. https://doi.org/10.5281/zenodo.4421777

Pika, P., Hulse, D., & Arndt, S. (2021). OMEN-SED(-RCM) (v1.1): A pseudo-reactive continuum representation of organic matter degradation dynamics for OMEN-SED. *Geoscientific Model Development*, *14*(11), 7155–7174. https://doi.org/10.5194/gmd-14-7155-2021

Pozzato, L., Cathalot, C., Berrached, C., Toussaint, F., Stetten, E., Caprais, J. C., et al. (2017). Early diagenesis in the Congo deep-sea fan sediments dominated by massive terrigenous deposits: Part I—Oxygen consumption and organic carbon mineralization using a micro-electrode approach. *Deep-Sea Research Part II Topical Studies in Oceanography*, *142*, 125–138. https://doi.org/10.1016/j.dsr2.2017.05.010

Rabouille, C., Gaillard, J.-F., Relexans, J.-C., Tréguer, P., & Vincendeau, M.-A. (1998). Recycling of organic matter in Antarctic sediments: A transect through the polar front in the Southern Ocean (Indian sector). *Limnology & Oceanography*, *43*(3), 420–432. https://doi.org/10.4319/lo.1998.43.3.0420

Rabouille, C., Olu, K., Baudin, F., Khripounoff, A., Dennielou, B., Arnaud-Haond, S., et al. (2017). The Congolobe project, a multidisciplinary study of Congo deep-sea fan lobe complex: Overview of methods, strategies, observations and sampling. *Deep Sea Research Part II: Topical Studies in Oceanography*, *142*, 7–24. https://doi.org/10.1016/j.dsr2.2016.05.006

Rice, A. L., Billett, D. S., Thurston, M. H., & Lampitt, R. S. (1991). The institute of oceanographic sciences biology programme in the porcupine seabight: Background and general introduction. *Journal of the Marine Biological Association of the United Kingdom*, *71*(2), 281–310. https://doi.org/10.1017/S0025315400051614

Riebesell, U., Schloss, I., & Smetacek, V. (1991). Aggregation of algae released from melting sea ice: Implications for seeding and sedimentation. *Polar Biology*, *11*(4). https://doi.org/10.1007/BF00238457

Ritzrau, W., Graf, G., Scheltz, A., & Queisser, W. (2001). Bentho-pelagic coupling and carbon dynamics in the northern North Atlantic. In *The northern north Atlantic* (Vol. 6, pp. 207–224). Springer Berlin Heidelberg. https://doi.org/10.1007/978-3-642-56876-3_13

Robador, A., Brüchert, V., & Jørgensen, B. B. (2009). The impact of temperature change on the activity and community composition of sulfate-reducing bacteria in arctic versus temperate marine sediments. *Environmental Microbiology*, *11*(7), 1692–1703. https://doi.org/10.1111/j.1462-2920.2009.01896.x

Røy, H., Kallmeyer, J., Adhikari, R. R., Pockalny, R., Jørgensen, B. B., & D'Hondt, S. (2012). Aerobic microbial respiration in 86-million-year-old deep-sea red clay. *Science*, *336*(6083), 922–925. https://doi.org/10.1126/science.1219424

Sachs, O., Sauter, E. J., Schlüter, M., Rutgers van der Loeff, M. M., Jerosch, K., & Holby, O. (2009). Benthic organic carbon flux and oxygen penetration reflect different plankton provinces in the Southern Ocean. *Deep Sea Research Part I: Oceanographic Research Papers*, *56*(8), 1319–1335. https://doi.org/10.1016/j.dsr.2009.02.003

Sagemann, J., Jørgensen, B. B., & Greeff, O. (1998). Temperature dependence and rates of sulfate reduction in cold sediments of Svalbard, Arctic ocean. *Geomicrobiology Journal*, *15*(2), 85–100. https://doi.org/10.1080/01490459809378067

Sauter, E. J., Schlüter, M., & Suess, E. (2001). Organic carbon flux and remineralization in surface sediments from the northern North Atlantic derived from pore-water oxygen microprofiles. *Deep Sea Research Part I: Oceanographic Research Papers*, *48*(2), 529–553. https://doi.org/10.1016/S0967-0637(00)00061-3

Savoye, B., Babonneau, N., Dennielou, B., & Bez, M. (2009). Geological overview of the Angola-Congo margin, the Congo deep-sea fan and its submarine valleys. *Deep Sea Research Part II: Topical Studies in Oceanography*, *56*(23), 2169–2182. https://doi.org/10.1016/j.dsr2.2009.04.001

Savoye, B., Cochonat, P., Apprioual, R., Bain, O., Baltzer, A., Bellec, V., et al. (2000). Structure et evolution recente de l'eventail turbiditique du Zaire: Premiers resultats scientifiques des missions d'exploration Zaiango 1 and 2 (marge Congo-Angola). *Comptes Rendus de l'Academie des Sciences - Series IIA: Earth and Planetary Science*, *331*(3), 211–220. https://doi.org/10.1016/S1251-8050(00)01385-9

Sayles, F. L., Deuser, W. G., Goudreau, J. E., Dickinson, W. H., Jickells, T. D., & King, P. (1996). The benthic cycle of biogenic opal at the Bermuda Atlantic Time Series site. *Deep-Sea Research Part I Oceanographic Research Papers*, *43*(4), 383–409. https://doi.org/10.1016/0967-0637(96)00027-1

Schlüter, M. (1991). Organic carbon flux and oxygen penetration into sediments of the Weddell Sea: Indicators for regional differences in export production. *Marine Chemistry*, *35*(1–4), 569–579. https://doi.org/10.1016/S0304-4203(09)90043-3

Seiter, K., Hensen, C., Schröter, J., & Zabel, M. (2004). Organic carbon content in surface sediments—Defining regional provinces. *Deep-Sea Research Part I Oceanographic Research Papers*, *51*(12), 2001–2026. https://doi.org/10.1016/j.dsr.2004.06.014

Seiter, K., Hensen, C., & Zabel, M. (2005a). Benthic carbon mineralization on a global scale. *Global Biogeochemical Cycles*, *19*(1), 1–26. https://doi.org/10.1029/2004GB002225

Seiter, K., Hensen, C., & Zabel, M. (2005b). Global data compilation of benthic data sets II [Dataset]. PANGAEA. (In supplement to: Seiter et al. (2005)). https://doi.org/10.1594/PANGAEA.143739

Smith, C. R. (1992). *Tempo and mode in deep-sea benthic ecology: Punctuated equilibrium revisited* (Vol. 6, p. 274). The Paleontological Society Special Publications. https://doi.org/10.1017/S2475262200008340

Smith, D. C., Simon, M., Alldredge, A. L., & Azam, F. (1992). Intense hydrolytic enzyme activity on marine aggregates and implications for rapid particle dissolution. *Nature*, *359*(6391), 139–142. https://doi.org/10.1038/359139a0

Smith, K. L., Kaufmann, R. S., & Baldwin, R. J. (1994). Coupling of near-bottom pelagic and benthic processes at abyssal depths in the eastern North Pacific Ocean. *Limnology & Oceanography*, *39*(5), 1101–1118. https://doi.org/10.4319/lo.1994.39.5.1101

Smith, K. L., Ruhl, H. A., Kahru, M., Huffard, C. L., & Sherman, A. D. (2013). Deep ocean communities impacted by changing climate over 24 y in the abyssal northeast Pacific ocean. *Proceedings of the National Academy of Sciences of the United States of America*, *110*(49), 19838–19841. https://doi.org/10.1073/pnas.1315447110

Soetaert, K., Herman, P. M., & Middelburg, J. J. (1996a). Dynamic response of deep-sea sediments to seasonal variations: A model. *Limnology & Oceanography*, *41*(8), 1651–1668. https://doi.org/10.4319/lo.1996.41.8.1651

Soetaert, K., Herman, P. M., & Middelburg, J. J. (1996b). A model of early diagenetic processes from the shelf to abyssal depths. *Geochimica et Cosmochimica Acta*, *60*(6), 1019–1040. https://doi.org/10.1016/0016-7037(96)00013-0

Ståhl, H., Tengberg, A., Brunnegård, J., & Hall, P. O. (2004). Recycling and burial of organic carbon in sediments of the porcupine Abyssal Plain, NE Atlantic. *Deep-Sea Research Part I Oceanographic Research Papers*, *51*(6), 777–791. https://doi.org/10.1016/j.dsr.2004.02.007

Stolpovsky, K., Dale, A. W., & Wallmann, K. (2015). Toward a parameterization of global-scale organic carbon mineralization kinetics in surface marine sediments. *Global Biogeochemical Cycles*, *29*(6), 812–829. https://doi.org/10.1002/2015GB005087

Takahashi, T., Broecker, W. S., & Langer, S. (1985). Redfield ratio based on chemical data from isopycnal surfaces. *Journal of Geophysical Research*, *90*(C4), 6907–6924. https://doi.org/10.1029/jc090ic04p06907

Thamdrup, B., & Fleischer, S. (1998a). Temperature dependence of oxygen respiration, nitrogen mineralization, and nitrification in Arctic sediments. *Aquatic Microbial Ecology*, *15*(2), 191–199. https://doi.org/10.3354/ame015191

Thamdrup, B., & Fleischer, S. (1998b). Temperature dependence of oxygen respiration, nitrogen mineralization, and nitrification in arctic sediments. *Aquatic Microbial Ecology*, *15*(2), 191–199. https://doi.org/10.3354/ame015191

Thiel, H. (1988). Phytodetritus on the deep-sea floor in a central oceanic region of the northeast Atlantic. *Biological Oceanography*, *6*(2), 203–239. https://doi.org/10.1080/01965581.1988.10749527

Thullner, M., Dale, A. W., & Regnier, P. (2009). Global-scale quantification of mineralization pathways in marine sediments: A reaction-transport modeling approach. *Geochemistry, Geophysics, Geosystems*, *10*(10), Q10012. https://doi.org/10.1029/2009GC002484

Thunell, R., Tappa, E., Varala, R., Llano, M., Astor, Y., Muller-Karger, F., & Bohrer, R. (1999). Increased marine sediment suspension and fluxes following an earthquake. *Nature*, *398*(6724), 233–234. https://doi.org/10.1038/18430

Toth, D. J., & Lerman, A. (1977). Organic matter reactivity and sedimentation rates in the ocean. *American Journal of Science*, *277*(4), 465–485. https://doi.org/10.2475/ajs.277.4.465

Tromp, T. K., Van Cappellen, P., & Key, R. M. (1995). A global model for the early diagenesis of organic carbon and organic phosphorus in marine sediments. *Geochimica et Cosmochimica Acta*, *59*(7), 1259–1284. https://doi.org/10.1016/0016-7037(95)00042-X

Ullman, W. J., & Aller, R. C. (1982). Diffusion coefficients in nearshore marine sediments. *Limnology & Oceanography*, *27*(3), 552–556. https://doi.org/10.4319/lo.1982.27.3.0552

Van Cappellen, P., & Wang, Y. (1996). Cycling of iron and manganese in surface sediments: A general theory for the coupled transport and reaction of carbon, oxygen, nitrogen, sulfur, iron, and manganese. *American Journal of Science*, *296*(3), 197–243. https://doi.org/10.2475/ajs.296.3.197

Van Mooy, B. A., Keil, R. G., & Devol, A. H. (2002). Impact of suboxia on sinking particulate organic carbon: Enhanced carbon flux and preferential degradation of amino acids via denitrification. *Geochimica et Cosmochimica Acta*, *66*(3), 457–465. https://doi.org/10.1016/s0016-7037(01)00787-6

Wadham, J. L., Arndt, S., Tulaczyk, S., Stibal, M., Tranter, M., Telling, J., et al. (2012). Potential methane reservoirs beneath Antarctica. *Nature*, *488*(7413), 633–637. https://doi.org/10.1038/nature11374

Washburn, L., Kadko, D. C., Jones, B. H., Hayward, T., Kosro, P. M., Stanton, T. P., et al. (1991). Water mass subduction and the transport of phytoplankton in a coastal upwelling system. *Journal of Geophysical Research*, *96*(C8), 14927. https://doi.org/10.1029/91jc01145

Wefer, G., & Fischer, G. (1991). Annual primary production and export flux in the Southern Ocean from sediment trap data. *Marine Chemistry*, *35*(1–4), 597–613. https://doi.org/10.1016/S0304-4203(09)90045-7

Wenzhöfer, F., Adler, M., Kohls, O., Hensen, C., Strotmann, B., Boehme, S., & Schulz, H. (2001). Calcite dissolution driven by benthic mineralization in the deep-sea: In situ measurements of Ca_2^+, pH, pCO_2 and O_2. *Geochimica et Cosmochimica Acta*, *65*(16), 2677–2690. https://doi.org/10.1016/S0016-7037(01)00620-2

Wenzhöfer, F., & Glud, R. N. (2002). Benthic carbon mineralization in the Atlantic: A synthesis based on in situ data from the last decade. *Deep-Sea Research Part I Oceanographic Research Papers*, *49*(7), 1255–1279. https://doi.org/10.1016/S0967-0637(02)00025-0

Wenzhöfer, F., Holby, O., & Kohls, O. (2001). Deep penetrating benthic oxygen profiles measured in situ by oxygen optodes. *Deep-Sea Research Part I Oceanographic Research Papers*, *48*(7), 1741–1755. https://doi.org/10.1016/S0967-0637(00)00108-4

Witte, U., Aberle, N., Sand, M., & Wenzhöfer, F. (2003). Rapid response of a deep-sea benthic community to POM enrichment: An in situ experimental study. *Marine Ecology Progress Series*, *251*, 27–36. https://doi.org/10.3354/meps251027

Witte, U., Wenzhöfer, F., Sommer, S., Boetius, A., Heinz, P., Aberle, N., et al. (2003). In situ experimental evidence of the fate of a phytodetritus pulse at the abyssal sea floor. *Nature*, *424*(6950), 763–766. https://doi.org/10.1038/nature01799

Zonneveld, K. A. F., Versteegh, G. J. M., Kasten, S., Eglinton, T. I., Emeis, K.-C., Huguet, C., et al. (2010). Selective preservation of organic matter in marine environments; processes and impact on the sedimentary record. *Biogeosciences*, *7*(2), 483–511. https://doi.org/10.5194/bg-7-483-2010